HHS Public Access

Author manuscript

Nat Struct Mol Biol. Author manuscript; available in PMC 2017 September 13.

Published in final edited form as:

Nat Struct Mol Biol. 2017 April ; 24(4): 419–430. doi:10.1038/nsmb.3389.

A mammalian nervous system-specific plasma membrane proteasome complex that modulates neuronal function

Kapil V. Ramachandran[1,*] and **Seth S. Margolis**[1,2,*]

[1]Department of Biological Chemistry, The Johns Hopkins University School of Medicine, Baltimore, Maryland, USA

[2]Solomon H. Snyder Department of Neuroscience, The Johns Hopkins University School of Medicine, Baltimore, Maryland, USA

Abstract

In the nervous system, rapidly occurring processes such as neuronal transmission and calcium signaling are affected by short-term inhibition of proteasome function. It remains unclear how proteasomes can acutely regulate such processes, as this is inconsistent with their canonical role in proteostasis. Here, we made the discovery of a mammalian nervous system-specific membrane proteasome complex that directly and rapidly modulates neuronal function by degrading intracellular proteins into extracellular peptides that can stimulate neuronal signaling. This proteasome complex is tightly associated with neuronal plasma membranes, exposed to the extracellular space, and catalytically active. Selective inhibition of this membrane proteasome complex by a cell-impermeable proteasome inhibitor blocked extracellular peptide production and attenuated neuronal activity-induced calcium signaling. Moreover, membrane proteasome-derived peptides are sufficient to induce neuronal calcium signaling. Our discoveries challenge the prevailing notion that proteasomes primarily function to maintain proteostasis, and highlight a form of neuronal communication through a membrane proteasome complex.

Introduction

Proteasomes are heterogeneous multisubunit catalytic complexes that consist of a core 20S stacked ring of α/β subunits with a $\alpha_7\beta_7\beta_7\alpha_7$ architecture, and can be associated with 19S regulatory cap-particles to form a 26S proteasome[1]. Among the other 20S-containing proteasomes are 20S proteasomes capped with 11S or PA200[1]. While capped 26S proteasomes mediate ATP-dependent degradation of ubiquitinated proteins, uncapped 20S

*To whom correspondence should be addressed: The Johns Hopkins University School of Medicine, Department of Biological Chemistry, Wood Basic Science Building Room 517, 725 North Wolfe Street, Baltimore, MD 21205, USA, Phone: 410-502-5362, Fax: 410-955-5759, kramach5@jhmi.edu and smargol7@jhmi.edu.

Author Contribution

K.V.R. and S.S.M. designed experiments. K.V.R. performed all experiments. K.V.R. and S.S.M. analyzed and interpreted the data and wrote the paper.

Competing financial interests

The authors declare no competing financial interests.

proteasomes do not require ubiquitin or ATP for their catalytic function[2–4]. Recent studies have shown that 20S proteasomes may have key biological functions separate from the canonical 26S ubiquitin-proteasome, particularly in clearing unstructured proteins and in degrading proteins during cellular stress[4].

20S proteasomes are absolutely essential in mammalian cells. In lieu of genetic perturbation, proteasome function has been studied through the use of many different inhibitors such as MG-132, Lactacystin, Epoxomicin, and peptide boronates[5]. The use of these inhibitors has revealed diverse roles for the proteasome in many different tissues and contexts, driven by protein homeostasis through ubiquitin-dependent proteasomal degradation. Typically, these processes require proteasome function over hours to days (long-term). Indeed, proteasomes do play such long-term roles in important aspects of neuronal function such as synaptic remodeling and cell migration[6,7]. However, proteasome function is also required for activity-dependent neuronal processes over very short timescales (seconds to minutes), such as regulating the speed and intensity of neuronal transmission or the maintenance of long-term potentiation, a molecular underpinning of learning and memory[6,8–13]. Presumably, short-term inhibition of the proteasome should not be able to meaningfully change the overall protein landscape, so it was unclear how proteasomes could rapidly alter neuronal function. Thus, we reasoned that an unidentified function for proteasomes in the nervous system must exist.

Changes in calcium dynamics and transients underlie many of these neuronal processes that occur over short timescales. Indeed, perturbation of proteasome activity has been shown to affect calcium dynamics in neurons[13,14]. Consistent with these findings, we observed that acute addition of the pan-proteasome inhibitor MG-132 onto neurons suppressed neuronal activity-induced calcium signaling (Supplementary Fig. 1). The effect on calcium dynamics that we observed occurred within seconds of MG-132 addition, indicative of a signaling role for proteasomes independent of their proteostatic role. Studies addressing the role for proteasomes in the nervous system have either used pan-proteasome inhibitors such as MG-132 or have focused on the 26S proteasome through altering the ubiquitination pathway[11,13,15]. These approaches do not distinguish between uncapped 20S or capped-20S proteasomes. We considered that evaluating proteasomes in the nervous system, without bias for 20S or 20S-containing proteasomes, would provide a means to identify unique proteasomes that could have acute signaling functions.

Results

20S proteasome subunits are localized to neuronal plasma membranes

Previous studies have identified localization as a key feature in determining proteasome function[16]. Distribution of the 26S proteasome in the nervous system has been measured using fluorescently-tagged 19S cap subunits or electron cryotomography (Cryo-ET)[10,17,18]. While cryo-ET approaches are theoretically unbiased, the processing methods inherently select for analysis of larger complexes, and therefore are more likely to identify singly- and doubly-capped proteasomes. In order to take a high resolution and unbiased approach to evaluate localization of all proteasomes (20S and 20S-containing) in the nervous system, we performed an immunogold electron microscopy (Immuno-EM) analysis of hippocampal

slice preparations using antibodies raised against either the proteasome β2, β5 or α2 subunits. These are core 20S proteasome subunits common to all catalytically active proteasomes[1,19].

We first performed western blot analysis of mouse brain lysates to assess the antibodies used for our immuno-EM studies. Brains from P30 mice were lysed and prepared for SDS-PAGE, and then immunoblotted using proteasome β2, β5, and α2 subunit antibodies. Each antibody recognized a single band by western analysis at the appropriate molecular weight (Fig. 1a–e). We proceeded to perform immuno-EM from mouse hippocampal sections using these antibodies and appropriate gold-conjugated secondary antibodies. We did not detect any significant staining using secondary gold-conjugated antibodies alone (Supplementary Fig. 2a–c). We observed diverse subcellular and cytosolic distribution of gold particles corresponding to proteasome subunits, as previously reported[1] (Fig. 1a–e and Supplementary Fig. 3a–c). Unexpectedly, we observed ~40% of all gold particles localized to neuronal plasma membranes (PM). Similar results were obtained using two additional antibodies raised against β2 and β5 subunits, but directed against different epitopes (Fig. 1b, 1d and Supplementary Fig. 3a, 3b). In contrast, we did not observe PM localization of gold particles when using antibodies raised against 19S cap proteins Rpt5 or S2 subunit (Fig. 1f and Supplementary Fig. 3d). Immunostaining using these 19S antibodies show diffuse cytosolic localization, consistent with prior studies[10].

Extending these findings, we performed immuno-EM analysis from mouse primary neuronal cultures, as these preparations are largely devoid of non-neuronal cell types and can provide higher resolution analysis[20,21]. No immunogold label was observed in samples treated with secondary gold-conjugated antibodies alone (Supplementary Fig. 4a). Using proteasome β2 and β5 subunit antibodies in mature cultured neurons, we observed ~40% of immunogold signal at neuronal PMs (Fig. 2a and Supplementary Fig. 4b). Of those particles observed at neuronal PMs, 43 ± 2% overlaid PMs, 38 ± 1.7% were located at the intracellular face, and 19 ± 2.4% were at the extracellular face (Fig. 2a). Using similar immuno-EM approaches, we did not observe PM localization of proteasomes in cultured non-neuronal HEK293 cells, which had particles localized to the cytoplasm (Supplementary Fig. 4c). Because conjugation of a primary antibody to a gold-particle tagged secondary antibody can result in the gold particle being localized up to ~20 nm from the target antigen, we quantified the fine localization of gold particles near neuronal PMs and plotted each particle in relation to its distance from the PM. This was a linear measurement taken from the center of the PM to the centroid of the gold particle. A majority of particles overlaid the PM, with the particle density diminishing as a function of distance from the membrane (Fig. 2b). Thus, the signal observed at plasma membranes corresponds to a unique pool of membrane-localized proteasome subunits rather than a reflection of intracellular proteasome subunits. Since core proteasome subunits are not known to be present in the cell separate from the macromolecular proteasome complex, these data likely reflected the membrane localization of intact proteasomes[1].

Neuronal membrane proteasomes are exposed to the extracellular space

Immuno-EM staining with a previously validated antibody raised against the cytoplasmic domain of the voltage-gated potassium channel, Kv1.3, only showed cytosolic labeling and labeling on the intracellular face of the PM as previously described[22] (Supplementary Fig. 5a). By immuno-EM analysis we see 20S proteasome staining on the extracellular face of the PM, which raises the possibility that proteasomes may be exposed to the extracellular space (Fig. 1a–e, 2a and Supplementary Fig. 3a–c, 4b). We decided to use three additional approaches to substantiate these findings: one specifically detecting proteasome subunits (antibody feeding) and two unbiased approaches to detect surface exposed proteins (surface biotinylation & protease protection) (Fig. 2c). First, we used antibody feeding onto live neuronal cultures[23,24]. No staining was observed using secondary alone controls (Supplementary Fig. 5b). Feeding a primary antibody against an N-terminal extracellular epitope of the GluR1 (N-GluR1) ionotropic receptor showed punctal staining as previously reported[25]. We did not observe staining upon feeding an antibody against intracellular protein MAP2 (Fig. 2d). Using the proteasome β5 subunit antibody, we observed punctal localization that was largely eliminated upon pretreatment of the β5 antibody with the β5 blocking peptide (Fig. 2d).

To biochemically determine whether proteasomes were surface-exposed, we turned to previously described surface-biotinylation/purification approaches[26,27] followed by immunoblotting with antibodies against Actin, GluR1, Rpt5 and 20S proteasome subunits. As expected, in our streptavidin pulldown samples from surface-biotinylated neurons we did not detect cytosolic Actin and did detect GluR1 (Fig. 2e). Consistent with 20S proteasomes being surface-exposed, we detected core 20S proteasome subunits in our streptavidin pulldown but did not detect significant pulldown of Rpt5 (Fig. 2e). Several measurements were taken to assure our results were not due to poor cell health or enhanced cell permeability (Supplementary Fig. 5c and 5d).

As an orthogonal method of identifying surface exposed proteins, we used a protease protection assay, which relies on the proteolysis of extracellularly exposed epitopes of proteins upon treatment of live cells with an extracellular protease[28,29]. Cultured cortical neurons were treated with Proteinase K (PK) for varying times and then fractionated into either cytosolic or membrane fractions. By immunoblot analysis, we found that proteasomes fractionated to the membrane, similar to N-GluR1, and were susceptible to proteolysis by extracellular PK (Fig. 2f). In contrast, proteasomes from the cytosolic fraction, similar to Tubulin, were protected from protease cleavage[30] (Fig. 2f). Because PK, when added to live cells can only degrade proteins exposed to the extracellular space, we interpreted this observation to mean that proteasomes were surface-exposed and that the majority of proteasomes in our membrane preparations are from plasma membranes and not from other membrane organelles. This result was corroborated using Concanavalin-A (ConA), a lectin binding protein that has been used to enrich plasma membranes[31] (Supplementary Fig. 5e). Taken together, these data support the existence of a surface exposed proteasome complex at the neuronal plasma membrane. For convenience, we will henceforth refer to the proteasome localized to the neuronal plasma membrane as the neuronal membrane proteasome, or NMP.

Neuronal membrane proteasomes are tightly associated with plasma membranes

We wanted to further enhance our biochemical understanding of how proteasomes, as largely hydrophilic complexes, could be localized to the hydrophobic PM. Neuronal membranes were isolated and sequentially extracted with increasing concentrations of digitonin to pull out increasingly hydrophobic proteins. Samples were prepared for western analysis (Fig. 3a). Quantification of these immunoblots revealed that a significant percentage of alpha and beta subunits co-fractionated with cytosolic proteins (Tubulin) and hydrophobic membrane proteins (GluR1). These data are consistent with proteasomes fractionating in two different modes, one that is cytosolic and another that is membrane-bound, providing additional evidence for a unique pool of membrane-localized proteasomes in contrast to cytosolic proteasomes (Fig. 3a). To determine whether NMPs were tightly or peripherally associated with plasma membranes, we used sodium carbonate extraction. Neuronal cultures were separated into cytosolic, peripherally-associated (carbonate-soluble) and tightly-associated (carbonate-insoluble) membrane protein fractions[29]. Calregulin[32] was used as a marker of peripherally-associated membrane proteins, whereas GluR1 was used as a marker of tightly-associated membrane proteins. Immunoblotting these fractions showed that core 20S proteasome components were tightly-associated (carbonate-insoluble), while Rpt5 was peripherally-associated (carbonate-soluble) (Fig. 3b).

We considered there were two primary ways this could be possible: (1) the proteasome itself was hydrophobic in some way or (2) the proteasome was tightly associating with integral membrane proteins. In an attempt to distinguish between these possibilities, we performed Triton X-114 (TX114) phase partitioning of cultured neurons to separate hydrophilic and hydrophobic proteins[33]. Immunoblotting the TX114-rich and TX114-free fractions, we observed Actin fractionated into the TX114-free phase, multi-pass transmembrane protein GluR1 fractionated into the TX114-rich phase, and EphB2, a single-pass transmembrane protein fractionated into both phases (Fig. 3c). Proteasome subunits fractionated in both phases, with only ~20–30% of proteasome subunits fractionating in the TX114-rich phase (Fig. 3c). Based on our immuno-EM, surface biotinylation, and membrane fractionation data, up to 40% of proteasome subunits were plasma membrane-localized. We reasoned that the discrepancy between these analyses might be due to the fact that proteasomes were not sufficiently hydrophobic to exist in the plasma membrane independent of auxiliary membrane proteins.

Neuronal membrane proteasomes are largely a 20S proteasome and in complex with GPM6 family glycoproteins

To identify potential auxiliary membrane proteins associated with the NMP we isolated proteasome complexes out of neurons using two different affinity methods[34]. Cytosolic and membrane-extracted fractions from neuronal cultures were incubated with 20S purification matrix (purifies any 20S-containing proteasome complex) or 26S purification matrix (only purifies 26S cap-containing proteasome complex). Immunoblot analysis revealed that both 20S and 26S affinity purification matrices isolated cytosolic proteasomes, but only the 20S purification matrix was able to purify proteasomes out of the membrane (Fig. 4a), suggesting to us that this is an approach for purifying the NMP.

Using the 20S-purification matrix, we purified 20S proteasomes from the cytosol and membrane of neurons for in-depth mass spectrometry (MS) analysis. As expected, we identified all of the core 20S proteasome subunits in the purification from both membranes and cytosol (Supplemental Table 1a). While we identified a variety of regulatory cap proteins to co-purify with the cytosolic proteasome, we identified very few to co-purify with the proteasome purified from membranes (Supplemental Table 1a). These findings were validated by extensive western analysis (Supplementary Fig. 6a–c).

We sought to identify auxiliary membrane proteins in our MS data sets that may be capable of mediating proteasome association with the plasma membrane. We postulated that such a protein would specifically associate with the NMP compared to the cytosolic proteasome, be highly expressed in the nervous system, and be transmembrane (Supplemental Table 1b). Based on these criteria, we focused our efforts on the neuronal membrane glycoprotein GPM6A, a known member of the Proteolipid Protein family of multi-pass transmembrane glycoproteins[35,36]. To validate these mass spectrometry data, we turned to HEK293 cells as a non-neuronal heterologous system that does not express the NMP (Supplementary Fig. 7a). Lysates from HEK293 cells previously transfected with expression plasmids encoding myc-/FLAG-tagged GPM6A and GPM6B (myc/FLAG-GPM6A/B) were immunoprecipitated using an anti-FLAG antibody. Immunoblotting using antibodies against myc and 20S proteasome subunits, we found that endogenous proteasome subunits from HEK293s co-immunoprecipitate with myc/FLAG-GPM6A/B (Fig. 4b). While we interpret these data to mean that proteasomes can associate with GPM6 proteins, as demonstrated from our MS data from neurons, we wanted to know whether the GPM6 proteins could induce the proteasome to become membrane-bound and surface-exposed. Using the surface biotinylation assay, we determined that expression of GPM6A and GPM6B in HEK293s was sufficient to induce surface expression of the endogenous HEK293 proteasome at the PM (Fig. 4c). These results are not seen upon overexpressing GFP, single-pass transmembrane protein EphB2, or multi-pass transmembrane protein Channelrhodopsin 2 (Fig. 4c). We uniformly detected the plasma membrane protein, Transferrin, verifying equal pulldown efficiency (Fig. 4c). Additionally, overexpression of myc-tagged β5 proteasome subunit together with myc/FLAG-GPM6A/B led to both myc-β5 and the endogenous subunits to become surface exposed (Fig. 4c). These findings phenocopy the phenomenon we observe in primary cultured neurons, and indicate the GPM6A/B proteins are sufficient to expose proteasomes to the extracellular space. Attempts to determine whether GPM6 family proteins were required for NMP expression were unsuccessful as shRNA-mediated knockdown of GPM6A in neuronal cultures induced cell death, suggesting GPM6 proteins may be essential for viability (data not shown).

GPM6A and GPM6B are primarily expressed in the nervous system[37]. Consistent with these data, using our surface biotinylation assay in whole mouse tissues, we determined that NMP expression was restricted to mouse neuronal tissues (Fig. 4d). Similar results were observed using human brain tissue (Supplementary Fig. 7b). These data prompted us to determine whether NMP expression was regulated and changed over neuronal development. Using our surface biotinylation assay in slice preparations from mouse brain, we determined that NMP expression paralleled *in vivo* expression patterns of GluR1, whose expression functionally correlates with critical stages in neuronal development[26] (Fig. 4e). Performing the same

experiments in neuronal cultures, we observed that the NMP was expressed in neurons at DIV8, but not prior (Supplementary Fig. 7c, 7d) in contrast to relatively constant total proteasome expression.

Neuronal membrane proteasomes degrade intracellular proteins into extracellular peptides

To test whether the NMP was catalytically active, we purified proteasomes from both the cytosol and neuronal plasma membranes using a 20S purification matrix and incubated them with SUC-LLVY-AMC, a substrate that fluoresces upon proteasomal chymotrypsin-like cleavage[38]. Addition of a low concentration of SDS to the reaction relieves the gating mechanism of the 20S proteasome without denaturing the 20S or 26S proteasome holocomplex[4]. Addition of SDS greatly stimulated the catalytic activity of membrane proteasomes and had little effect on cytosolic proteasome activity (Fig. 5a and Supplementary Fig. 8a), consistent with a large fraction of NMPs being 20S and catalytically active.

We were curious as to the purpose of a surface-exposed catalytically active 20S proteasome in the neuronal plasma membrane. Since the core 20S complex alone is ~11×15 nm, any orientation of the NMP at the neuronal PM, which is 6–10 nm across, would provide it access to both the intracellular and extracellular space. We hypothesized that in neurons, a catalytically active proteasome in such an orientation would be able to promote proteasome-dependent degradation of intracellular proteins into the extracellular space. To test this hypothesis, we used ^{35}S-methionine/cysteine-radiolabelling approaches to trace the fate of newly synthesized intracellular proteins[39] (Fig. 5b). After 10 minutes of radiolabel incorporation (Fig. 5c), free radioactivity was washed away, and media was collected over a timecourse and analyzed by liquid scintillation to detect radiolabeled proteins. We observed rapid release of radioactivity into the culture medium under baseline conditions (Fig. 5d). We observed a significant decrease in radioactive flux following addition of MG-132, without affecting radiolabelling efficiency (Fig. 5c, 5d). Addition of ATPγS, a non-hydrolyzable ATP analog, had no effect on release of radioactive material (Fig. 5d). This was consistent with the release of radioactivity being due to an uncapped 20S proteasome, which does not require ATP. To determine whether the released radiolabel was incorporated into protein peptides, different fractions from the media were treated with PK to breakdown peptidergic material into single amino acids and dipeptides. Of the released radioactive material at the 2-minute collection time, 82 ± 5% was made up of PK-sensitive molecules that ranged between 500 and 3000 Daltons in size (Fig. 5e). Similar results were observed at a 30-minute collection time (Supplementary Fig. 8b). Since proteasome cleavage products are peptides between 500 and 3000 Da in size, we conclude that a large fraction of radioactivity in the media was composed of protein peptides derived from a proteasome[40] and not individual amino acids or small molecules. To discriminate between cytosolic and membrane proteasomes in mediating the efflux of extracellular peptides, we took advantage of the temporal switch in NMP expression between DIV7 and DIV8, where both DIV7 and DIV8 neurons express cytosolic proteasomes but only DIV8 neurons express the NMP (Supplementary Fig. 7c, 7d). We observed that proteasome-dependent release of radiolabeled peptides into the media was observed at DIV8, but not at DIV7, which paralleled the temporal expression of the NMP (Fig. 5f). Consistent with this being an NMP-

mediated neuronal phenomenon, we did not observe proteasome-dependent release of radiolabeled peptides in heterologous HEK293 cells that do not express the NMP (Supplementary Fig. 8c). Taken together, these data support our hypothesis that the NMP degrades intracellular proteins into extracellular peptides.

Neuronal membrane proteasomes are required for release of extracellular peptides and modulate neuronal activity

To specifically determine the contribution of the NMP in the generation of these extracellular peptides, separately from that of the cytosolic proteasome, we identified a chemical tool that was selective to the NMP. We found that biotinylation of the non-reactive portion of epoxomicin, a highly potent and specific proteasome inhibitor, generates a cell-impermeable compound (biotin-epoxomicin) that maintains target specificity[41]. This compound covalently modifies the catalytic proteasome β subunits, tagging them with biotin. Cultured neurons acutely treated with biotin-epoxomicin were separated into cytosolic and membranes fractions, and immunoblotted using streptavidin-AF647. Biotin signal was only observed in membranes from neurons treated with biotin-epoxomicin and at a size denoting the covalent modification of the membrane proteasome β subunits (Fig. 6a).

Furthermore, Immuno-EM analysis of neuronal cultures treated with biotin-epoxomicin showed 92 ± 5% of biotin at plasma membranes (Fig. 6b and Supplementary Fig. 9a). Any cytosolic labeling was likely due to streptavidin-Au binding endogenously biotinylated proteins, as we detected low-abundance cytosolic labeling in cultures not treated with biotin-epoxomicin (Supplementary Fig. 9a, 9b). Since biotin was directly labeled using streptavidin-Au, this analysis reduces the distance between the gold particle and the target antigen compared to conventional antibody-based immuno-EM. These data show that NMPs overlay neuronal plasma membranes and are exposed to the extracellular space and provide further evidence that the NMP is catalytically active, since epoxomicin requires proteasome activity in order to bind to and inhibit the catalytic subunits[42]. These data established biotin-epoxomicin as a useful tool for studying the relevance of the NMP.

Using this inhibitor, we sought to separate the role of the NMP from the role of the cytosolic proteasome in regulating extracellular peptide production. Acute application of biotin-epoxomicin to radiolabeled neurons inhibited radioactive peptide release into the extracellular space (Fig. 6c). Using biotin-epoxomicin, we wanted to test our initial hypothesis that the NMP could mediate rapid neuronal signaling. To test whether the NMP was relevant to aspects of neuronal signaling, changes in intracellular calcium were measured since calcium serves as a rapid readout for many types of neuronal signaling[43]. Calcium imaging was performed using GCaMP3-transfected cultured neurons treated with perfusate containing GABAergic receptor antagonist bicuculline which, by relieving inhibition on neuronal circuits, induces regular firing of action potentials and calcium transients[43]. Following 2 minutes of bicuculline stimulation, perfusate was switched to buffer containing both bicuculline and 25 μM biotin-epoxomicin. Within 10–30 seconds of biotin-epoxomicin addition, we observed a rapid and robust attenuation of the amplitude of bicuculline-induced calcium transients, similar to that which we observed upon acute addition of MG-132 (Fig. 6d and 6e). Addition of biotin-epoxomicin induced a large

variability in the frequency of calcium transients: 47% of neurons displayed an increase in frequency, while the same treatment induced a potent abrogation of bicuculline-induced calcium signals in 31% of neurons (Fig. 6f). Based on these data, an endogenous function of the NMP is to modulate the strength and speed of activity-dependent neuronal signaling through its proteolytic activity, possibly through the actions of the resulting extracellular peptides.

Neuronal membrane proteasome-derived peptides are sufficient to induce neuronal signaling

To systematically test the effects of proteasome-directed peptide signaling, peptides were purified and then perfused onto GCaMP3-encoding neurons under various conditions. Neurons were ensured to be healthy at the end of every experiment by stimulating with 55 mM KCl, which consistently induced strong calcium signaling. The proteasome-directed peptides were purified and lyophilized following extensive dialysis into ammonium bicarbonate to remove small molecules and neurotransmitters. The lyophilizate was resuspended in calcium imaging buffer. Peptide concentration was determined to be ~50 ng/mL and was added back at that concentration. Alone, purified peptides induced a robust degree of calcium signaling in naïve neurons (Fig. 7a). This peptide-induced stimulation was eliminated if the peptide purification was done in the presence of PK (Fig. 7b). These data suggest that the observed calcium-signaling effects were due to the actions of extracellular protein peptides, and not small molecules or excitatory amino acids. Moreover, media collected in the presence of MG-132 did not possess the capacity to stimulate naïve neuronal cultures (Fig. 7c), indicating that the relevant bioactive peptides were derived from the proteasome. Moreover, in similar experiments, addition of random peptides to GCaMP3-encoding neurons did not possess the capacity to stimulate naïve neuronal cultures (Supplementary Fig. 10). We then determined that these peptides were inducing calcium flux from the outside of the cell in, rather than promoting release from intracellular calcium stores. Addition of cell-impermeable calcium chelator BAPTA to the perfusate abrogated the peptide-induced calcium signal (Fig. 7d), whereas depletion of ER calcium stores using thapsigargin did not reduce the maximum amplitude of the peptide-induced calcium signal (Fig. 7e).

To identify which channels were relevant to peptide-induced calcium activity, we used different ion channel inhibitors to pharmacologically identify relevant pathways. Blocking fast voltage-gated sodium channels using Tetrodotoxin did not block the peptide-induced calcium signal, revealing that the influx of calcium was probably not due to action potential-induced signaling, and more likely directly due to effects on calcium channels (Fig. 7f). Blockade of L-type calcium channel dependent influx using Nifedipine also did not modulate the peptide-induced calcium signal (Fig. 7g). However, inhibiting N-methyl-D-aspartate receptors (NMDARs) using 2-amino-5-phosphonopentanoic acid (APV) reduced the maximum amplitude of the peptide-induced calcium influx (Fig. 7h). Together, these data suggest that the peptides derived from the neuronal membrane proteasome can modulate neuronal activity, at least in part by driving calcium influx through NMDARs (Fig. 7i).

Discussion

We report on an unusual finding of a 20S proteasome that is tightly associated with the neuronal plasma membrane and exposed to the extracellular space. In this capacity, it can degrade intracellular proteins into bioactive extracellular peptides that induce calcium signaling through NMDA receptors. The model we prefer (discussed further below) based on these data are that a 20S proteasome complex is coupled to the plasma membrane by GPM6 glycoproteins, and that the extracellular peptides generated are the means by which the NMP acutely regulates neuronal function.

Proteasome association with neuronal plasma membranes and surface-exposure by GPM6 family glycoproteins

Identification of the GPM6 glycoprotein family as proteins that interact with proteasomes and are sufficient to induce the expression of proteasomes at the plasma membrane provides some insight into how proteasomes, as hydrophilic protein complexes, could interact so tightly with the hydrophobic plasma membrane. However, we noticed that the magnitude to which GPM6-induced membrane proteasome expression in heterologous cells did not match the magnitude of endogenous membrane proteasome expression in neurons. This suggests that there may in fact be other proteins that mediate the interaction of the NMP with the membrane, an area being actively investigated.

We postulate that the GPM6 glycoproteins may form a protein pore, perhaps through oligomeric interactions, which have been proposed previously[35,44]. In the right conformation, proteasomes binding to pore-containing membrane proteins could give proteasomes a hydrophilic binding surface to the hydrophobic plasma membrane, allowing the proteasome to gain access to the extracellular space. We propose a few models for how GPM6 proteins, or other membrane tethers may localize the proteasome to the plasma membrane (Fig. 8). In each case, we posited that 1) proteasomes must be located at plasma membranes, 2) proteasomes were in some fashion bound to auxiliary membrane proteins such as GPM6, and 3) proteasomes must be able to degrade proteins from the intracellular to the extracellular space. Model 1 – Cytoplasmic docking: In this model, a proteasome located at the plasma membrane would be docked on or tethered to auxiliary membrane proteins on the cytoplasmic side of the membrane. Degraded proteins would be shed through a peptide pore formed by the auxiliary proteins. Model 2 – Extracellular docking: In this model, a proteasome located at the plasma membrane would be docked on or tethered to auxiliary membrane proteins on the extracellular side of the membrane. Proteins would be delivered through a protein pore formed by the auxiliary proteins. Model 3 – Intramembrane docking: In this model, a proteasome located at the plasma membrane would be tethered or anchored to auxiliary membrane proteins within the lipid bilayer. The cell biological conundrum of how a proteasome can interact with the plasma membrane may be the most significant question to address in order to gain a deeper understanding of NMP function. Because antibody feeding and protease protection require that large molecules gain access to the proteasome, we posit that model 1 is less likely, and either model 2 or model 3 will prevail. While we find these models most consistent with our data, we certainly do not preclude

other potential models. Ultimately, the nature of this seemingly transmembrane complex can only be validated by a structural approach.

NMP composition and regulation

We made significant attempts to identify NMP interacting partners in an effort to determine whether the NMP was capped by the 19S, 11S, or PA200 subunits. Our data likely preclude the presence of the canonical 19S proteasome cap, or regulatory caps such as 11S or PA200[4,45,46]. While we identified a few 19S subunits co-fractionating with the NMP by mass spectrometry, we could not identify significant amount of key 19S subunits Rpt5 or S2. We also made the intriguing observation that immunoproteasome subunit PSMB8 uniquely co-fractionated with the NMP. Our finding that the NMP is likely a 20S core proteasome lacking the 19S cap is significant for two primary reasons. First, while a few functions for 20S proteasomes have been ascribed, their function independent of the 19S cap largely remains a mystery, especially in the nervous system[46]. Second, significant implications come from the idea that 20S proteasomes are primarily tasked with clearing misfolded or unstructured proteins[4,47,48]. A large source of disordered or unfolded proteins is derived from failed products of protein translation and misfolded or improperly folded proteins. These end-products of proteotoxic stress are hallmarks of many neurodegenerative disorders[49,50], a fact which places the NMP at the heart of various disease states.

NMP-directed peptide signaling modulates neuronal function

Unconventional secretion pathways have been implicated in release of cellular protein cargos[51,52]. Moreover, many groups have demonstrated that inhibition of ubiquitin-dependent proteasome function affects synaptic signaling and transmission. Our data support a role for the existence of a specialized neuronal membrane proteasome that mediates neuronal function by “inside-out” signaling through the production of extracellular proteasome-derived peptides. While it remains possible, we have not detected any role for secretion pathways or ubiquitin in the release of these peptides (Ramachandran and Margolis, unpublished data).

Proteasome-derived peptides, which when purified, rapidly and robustly stimulate neurons. Pharmacological dissection of the downstream pathways of peptide signaling revealed that NMP-derived peptides act in part by modulating NMDARs. The signaling through NMDARs only makes up ~50% of the total activity of the peptides. Other possible targets include: 1) Peptides interact with major histocompatibility immune complexes (MHC) that have recently been shown to play key roles in developmental and experience-dependent mechanisms in the nervous system[53,54]; 2) peptides modulate metabotropic ion channels, thereby altering calcium-mediated signaling; and/or 3) peptides signal to neuronal or non-neuronal cells such as glial cells through yet to be identified receptors.

It is well-established that NMDARs are critical for neuronal activity-dependent signaling relevant to learning and memory[55–57]. Given that cytosolic proteasomes have been shown to be regulated by neuronal activity, it will be intriguing to better understand whether the NMP and the resulting extracellular peptides are also modulated by changes in neuronal activity. It is also unclear how this signaling is specified within the brain, but we postulate that it relies

on how the NMP recognizes and targets proteins for degradation. Therefore, it will be critical to identify not only the sequences of the peptides, but also the substrates from which they are derived. These insights into substrate identity and targeting will reveal how the NMP functions, but may begin to link proteostatic failure under pathological conditions to NMP dysfunction.

Data Availability Statement

All reagents and protocols used in this study are available for sharing upon reasonable request to the authors. Source data for Figures 1,2,3,4,5,6, and 7 as well as mass spectrometry data are available online.

Online Methods

Antibodies

The following were used according to manufacturer's and/or published suggestions for western blotting and immunocytochemistry: anti-α1–7 proteasome subunit (Enzo), anti-α2 proteasome subunit (Cell Signaling), anti-α5 proteasome subunit (Santa Cruz), anti-β1 proteasome subunit (Santa Cruz), anti-β2 proteasome subunit (Santa Cruz), anti-β2 proteasome subunit (Enzo), anti-β2 proteasome subunit (Novus), anti-β2 proteasome subunit (Santa Cruz), anti-β5 proteasome subunit (Santa Cruz), anti-β5 proteasome subunit (Enzo), anti-Rpt5 proteasome subunit (Enzo), anti-calregulin (Santa Cruz), anti-β-Actin (Abcam), anti-Biotin (Cell Signaling), Streptavidin-AF647 (Invitrogen), anti-Tubulin (Milipore), anti-GluR1 (Cell Signaling), anti-Myc (Abcam), anti-Transferrin (Invitrogen), anti-EphB2 (M. Greenberg)[58], anti-NGluR1 (R. Huganir), cleaved Caspase-3 (Cell Signaling), anti-Kv1.3 (NeuroMab), anti-S2 (Milipore), anti-PA200 (Novus), anti-11Sα (Cell Signaling), anti-11Sβ (Cell Signaling). Antibodies obtained from commercial vendors were verified for specificity using western blotting, immunofluorescence, or immunoprecipitation. We prioritize those antibodies with a continued record of use in multiple independent studies (Supplementary Table 2). For proteasome antibodies, many antibodies used recognize a single band or set of bands at the known molecular weight. Genetic validation of these antibodies is impossible as all proteasome subunits are essential and no knockout controls can be obtained.

Mice

All animal procedures were performed under protocols compliant and approved by the Institutional Animal Care and Use Committees of The Johns Hopkins University School of Medicine. No difference was observed in experiments performed distinguishing between sexes. As such, both male and female mice were considered for analyses for this study. For all experiments, we use wild-type C57BL/6 mice (stock number 027 from Charles River Laboratories). These are general-use animals that are used by many laboratories in the field. The specific age of animal used is listed in the experimental procedure sections. For the majority of experiments, mice were euthanized with carbon dioxide-induced anoxia and decapitated as a secondary method of euthanasia. For in vivo experiments, animals were anesthetized with Isofluorane and then decapitated.

Perfusion

P30 WT C57Bl/6 Mice were anesthetized with Isoflourane and rapidly perfused with phosphate buffer and 0.5% paraformaldehyde/1.0% glutaraldehyde and brains were thin-sectioned for Immuno-EM analysis.

Immuno-electron microscopy and analysis

Brain slices from perfused mice and neuronal cultures were fixed and processed for Electron Microscopy. EM Grids were incubated in the primary antibody overnight at 4 °C followed by secondary antibodies for 2 hours at room temperature. All grids were viewed with a Phillips CM 120 TEM operating at 80 Kv and images were captured with an XR 80–8 Megapixel CCD camera by AMT. Neuronal cultures were fixed in 1.5% glutaraldehyde (EM grade, Pella) buffered with 70 mM sodium cacodylate containing 3 mM MgCl2 (356 mOsmols pH 7.2), for 1 hour at room temperature. Thin-sectioned fixed brain slices and neuronal cultures were processed using the following protocol. Following a 30 minute buffer rinse (100 mM cacodylate, 3% sucrose, 3 mM MgCl2, 316 mOsmols, pH 7.2), samples were post-fixed in 1.5% potassium ferrocyanide reduced 1% osmium tetroxide in 100 mM cacodylate containing 3 mM MgCl2, for 1 hr in the dark at 4 °C. After en-bloc staining with filtered 0.5% uranyl acetate (aq.), neurons were dehydrated through graded series of ethanols and embedded/cured with Eponate 12 (Pella). LR-white procedural staining was used for HEK293 cells as well as neuronal cultures (Supplementary Fig. 4C). A metal hole punch was used to remove 5 mm discs from the polymerized plates. Discs were mounted onto epon blanks and trimmed. Sections were cut on a Reichert Ultra cut E with a Diatome diamond knife. 80 nm sections were picked up on formvar coated 200 mesh nickel grids and treated for antigen removal followed by on grid immunolabelling. Grids were floated on 95 °C citrate buffer pH 6.0 in a porcelain staining dish for 25 minutes, and then allowed to cool on the same solution for 20 min. After a brief series of 50 mM TBS rinses, grids were floated on 50 mM NH4Cl in TBS, blocked with 2% horse serum in TBS (no tween) for 20 minutes. Grids were incubated in primary antibody diluted in blocking solution (1–50 Goat, mouse, rabbit antibody). Grids incubated on blocking solutions served as negative controls. Sections were allowed to come to room temperature (1 hour) on antibody solutions and placed on appropriated blocking solutions for 10 min. After further TBS rinses, grids were floated upon 12 nm Au conjugated donkey anti-goat, 12 nm Au conjugated goat anti-rabbit, 12 nm Au conjugated donkey anti-mouse, or Au conjugated streptavidin (Jackson Immunoresearch) at 1–40 dilutions in TBS for 2 hours at room temperature. Grids were then rinsed in TBS, floated upon 1% glutaraldehyde for 5min, rinsed again and stained with 2% filtered uranyl acetate. All grids were viewed with a Phillips CM 120 TEM operating at 80 Kv and images were captured with an XR 80–8 Megapixel CCD camera by AMT.

Cell lines

For primary mouse neuronal cultures, pregnant wild-type C57/B6 mice were obtained from Charles River Laboratories, and sacrificed at E17.5. Whole cortices were dissected, processed into a single cell suspension, and plated as previously described[58]. Primary cell lines isolated in our laboratory from mouse brains are identified by surface markers that are unique to neuronal cells. These approaches have high sensitivity to accurately identify

specific cells. Alternatively, for biochemical studies analysis of primary cell lines can be done using western blotting with well-validated antibodies to neuronal specific markers. Human Embryonic Kidney (HEK293) and Neuro-2A neuroblastoma cells were obtained from ATCC and maintained and expanded and frozen down in a series of aliquots. These aliquots are cultured for a limited number of passages (<10). They are regularly tested for any infection. The lab maintains strict guidelines for cell culture and monitoring of cell health in order to minimize biological variability and to prevent cell line cross-contamination during culture. Each cell line is maintained in its own culture medium.

Cell culture and Transfection

HEK293 and Neuro2A cells were cultured in DMEM supplemented with 10% fetal bovine serum, 2 mM glutamine (Sigma), and penicillin/streptomycin (100 U/mL and 100 μg/mL, respectively; Sigma). Mouse cortical neurons were prepared from E17.5 C57Bl/6 mouse embryos as previously described[58]. Neurons were maintained in Neurobasal Medium (Invitrogen) supplemented with 2% B-27 (Invitrogen), penicillin/streptomycin (100 U/mL and 100 μg/mL, respectively), and 2 mM glutamine. Dissociated neurons were transfected using the Lipofectamine method (Invitrogen) according to the manufacturer's suggestions.

Antibody feeding and immunocytochemistry

Cultured cortical neurons were plated on glass coverslips coated with poly-L lysine overnight. Neurons were allowed to mature to DIV 14 for feeding experiments. DIV 14 cortical neurons were slowly washed twice with cold PBS supplemented with 1 mM $CaCl_2$ and 2 mM $MgCl_2$ to slow recycling and internalization. Care was taken not to shear cell bodies from the neuron, and to maintain neuronal morphology. Cold neurons, while alive, were treated with Chicken anti-MAP2 antibodies (1:100), Goat anti-β5 proteasome subunit antibodies (1:50), and Rabbit anti-GluR1 (1:100) in PBS supplemented with 1mM $CaCl_2$ and 2 mM $MgCl_2$ for 30 minutes at 4°C. Antibodies were washed off, and neurons were rinsed twice in cold PBS, 1 minute each. Neurons with bound antibodies were fixed in 4% paraformaldehyde/4% sucrose in PBS for 75 seconds, so not to destroy the antibody itself but to maintain neuronal morphology. Samples were visualized using donkey anti-goat AF-488, donkey anti-chicken AF-555, and donkey anti-rabbit AF-647 (1:250 each) in 1× non-permeabilizing GDB (30 mM phosphate buffer pH 7.4 containing 0.2% gelatin, and 0.8 M NaCl) for 1 hour at 25 °C. Samples on coverslips were mounted on glass slides using Fluoromount-G (Southern Biotech). Neurons were imaged using a laser scanning Zeiss LSM780 FCS microscope. Images are representative maximal Z projections of multiple optical sections.

Protease protection assay

Cortical neuronal cultures were treated for the indicated times with 1 μg/mL of Proteinase K (NEB) in HBSSM (Hank's Balanced Salt Solution without $CaCl_2$ or phenol red, supplemented with 1 mM $MgCl_2$). Excess Proteinase K was quickly washed away three times in HBSSM, and Proteinase K activity was quenched twice for 3 minutes with 10 μM PMSF in HBSSM at 4 °C. Neurons were then fractionated into cytosolic and membrane fractions as described above, and samples were prepared for SDS-PAGE and western analysis.

Surface biotin-labeling, Cell lysis, streptavidin pulldown, and western blots

Surface biotin-labeling was performed as previously described [26]. Whole mouse brains, cultured cells or whole animal tissue were obtained where indicated and each sample was labeled using Sulfo-NHS-LC-Biotin (ThermoFisher). Cultured cells were washed in pH 8.0 PBS (Gibco) with 1 mM CaCl2 and 2 mM $MgCl_2$ (PBSCM) and treated with 1 mg/mL Sulfo-NHS-LC-Biotin dissolved in PBSCM for 20 minutes at 4 °C before the reaction was quenched for 10 minutes in 50 mM glycine in PBSCM. Intact tissue was quickly and manually chopped, following biotinylation for only 10 minutes at 4 °C in 0.5 mg/mL Sulfo-NHS-LC-Biotin prior to quenching the reaction. Whole mouse tissues and cultured neurons were collected and homogenized in RIPA buffer (50 mM Tris pH 8.0, 150 mM NaCl, 1% Triton X-100, 0.5% Sodium Deoxycholate, 0.1% SDS, 5 mM EDTA, complete protease inhibitor cocktail tablet (Roche), 1 mM β-glycerophosphate). Where indicated, the salt concentration in our RIPA lysis buffer was increased up to 300 mM NaCl. Primary, human central nervous system (CNS) tissue, gestational weeks 19–21, were obtained under surgical written consent following protocols approved by the Johns Hopkins Institutional Review Board, based on its designation as biological waste. Tissue was mechanically chopped at 4°C, and immediately processed for surface biotinylation. For streptavidin pulldown experiments, lysed cells were incubated with high-capacity streptavidin agarose beads (ThermoFisher) overnight and then washed thrice with RIPA buffer before elution in SDS sample buffer. Western blots were performed using conventional approaches. Gels were run either on 4–15% SDS-PAGE gradient gels (Bio-Rad) or on 10% gels made in the laboratory. Proteins were transferred to nitrocellulose membranes at 100V for 1.5 hours in 20% methanol containing transfer buffer. All antibodies were made up in 5% BSA in 0.1% TBST. Western blots were incubated with appropriate secondary antibodies coupled to Horseradish Peroxidase, extensively washed, and incubated with ECL. Images were exposed on film, and were scanned in and quantified using ImageJ by standard densitometry analysis.

Cellular Fractionation and integral membrane determination

For cellular fractionation experiments to determine the membrane attachment of the proteasome, cultured neurons were lysed in either a sucrose buffer (0.32 M sucrose, 5 mM HEPES, 0.1 mM EDTA, 0.25 mM DTT) or hypotonic lysis buffer (5 mM HEPES, 2 mM ATP, 1 mM $MgCl_2$) collected. Nuclei were pelleted at 800 RPM for 5 minutes, and the supernatant containing membranes was pelleted at 55000 RPM for 1 hour. Pelleted membranes were washed twice by homogenizing in lysis buffer and re-pelleted. Following two washes, membranes were processed for appropriate application. Supernatants containing the cytosolic extracts were concentrated down to the same volume that membranes were eventually resuspended in. Membrane association was determined by classic methods of sodium carbonate extraction. Briefly, purified neuronal membranes were resuspended in 50 mM sodium carbonate, pH 11 and incubated for 10 minutes at 4 °C to strip away membrane-associated proteins. Membranes, along with tightly-associated membrane proteins, were pelleted at 55000 RPM for 1 hour. Incubating membranes with sodium carbonate at high pH is thought to strip peripherally-associated proteins from the membranes, leaving only tightly-associated and integral membrane proteins bound to the membranes. Samples were subsequently prepared for SDS-PAGE analysis. For Digitonin fractionation, samples were lysed in sucrose buffer. Once the supernatant (cytosolic fraction) was set aside, the pellet

was washed 2x with sucrose buffer, and then resuspended in sucrose buffer with indicated concentrations of digitonin. Following a 30 minute incubation in the buffer, samples were spun down at 55000 RPM for 1 hour. This was repeated for all indicated concentrations of detergent. For Fig. 3A, based on our fractionation protocol, we calculated that the input was about 60% cytosol and 40% membrane. We only collected the non-nuclei, non-mitochondria membrane (i.e. 20% of remaining membranes). For our westerns in Fig. 3A we used 10 μl of input and ~3x-purified cytosol and ~5x-purified membrane. Combining the data from the cytosol and membrane fractions and considering error in our experimental approach proteasome signal from our input is likely coming from both the cytosol and a larger fraction from the membrane preparations. Because our input includes all the cellular material and the fractionation removes the nuclei and mitochondria we believe, if any, a very small amount of proteasome signal in our input can account for that which is coming from these organelles.

TX-114 phase extraction

Protocol was adapted from[33]. Briefly, primary neuronal cultures were treated with 1% precondensed TX-114. Samples were dounce homogenized, spun at 4°C, and incubated at 30 °C. Samples were centrifuged for 3 minutes at room temperature. Supernatant was retained as the TX114-free fraction and resulting pellet was kept as the TX114-rich fraction. This approach relies upon a temperature-dependent shift of the critical micellar concentration of TX-114, and provides an approximate determination of the hydrophobicity of proteins.

Concanavalin-A plasma membrane isolation

Protocol was adapted from[31]. Briefly, 0.25 mg biotinylated Concanavalin-A (ConA) was first coupled to 1 mL of streptavidin-coated agarose beads. Nuclei were pelleted from hypotonically lysed DIV 16 cultured cortical neurons, as described above, and the supernatant containing plasma membranes and cytosol were applied to 150ul of ConA beads. After thorough washing in lysis buffer containing 0.025% Nonidet-P40, samples were prepared for SDS-PAGE and western analysis.

DNA Constructs

The full-length mouse tagged GPM6A, tagged GPM6B, tagged β5 constructs were acquired from Origene. All vectors obtained from commercial sources are verified and tested for the appropriate expression of the inserts using primary antibodies or epitope-tag antibodies against the expressed proteins. While we keep stocks of each validated plasmid, we periodically sequence these plasmids to confirm their authenticity. All plasmids used in this study are amplified and purified using standard kits from commercial vendors.

shRNA Knockdown

Four unique shRNA constructs were obtained each against GPM6A, GPM6B, and PLP from Origene. These were validated HuSH 29mer shRNA constructs expressing GFP. Each construct was transfected into neurons using previously described and standard protocols. Each construct was transfected at 100 ng and 500 ng/well. In addition, the constructs were co-transfected in combination to knockdown either two, or all three genes.

Human Subjects

Fetal brain tissue was obtained at Johns Hopkins University. Primary cultures of fetal cortical tissues were prepared. The use of fetal brain tissue was approved by the Johns Hopkins University institutional review board (IRB). Informed consent was obtained from all subjects. The authors did not have access to any identifying personal information.

Co-immunoprecipitations

Transfected HEK293 cells were collected and homogenized in IP Buffer (1% NP-40, 2mM $MgCl_2$, 300mM NaCl, 2mM $CaCl_2$, 50mM HEPES, 10% Glycerol) buffer. For immunoprecipitations, lysates were incubated with FLAG-M2 agarose beads (Sigma-Aldrich). Precipitated samples were washed and prepared for SDS-PAGE and immunoblot analysis.

Proteasome purification and assessment of catalytic activity

For proteasome purification, cells were treated and then immediately put on ice before purifications were performed as previously described[45]. Briefly, proteasomes were purified out of neuronal cytosol and detergent-extracted neuronal plasma membranes using the 20S proteasome purification kit (Enzo Life Sciences) or the 26S proteasome purification kit (UBPBio). The first method relies on immunoprecipitating proteasomes using proteasome β5 subunit antibodies covalently coupled to agarose beads (20S purification matrix). It is important to note that this purification scheme can purify any 20S-containing proteasome complex. As an alternative method, we used a previously described affinity purification that utilizes GST-Ubl binding to the 19S cap and subsequent pulldown on Glutathione-coupled sepharose (26S purification matrix). This method enriches for proteasomes that are capped by the 19S complex. For western blots, samples were denatured at 65 °C for 5 minutes in SDS sample buffer, resolved by SDS PAGE, transferred to nitrocellulose, and immunoblotted. For catalytic activity assays, 1/6th of the bead volume following proteasome purification was resuspended in activity assay buffer (20 mM Tris-HCl, pH8.0, 5 mM ATP, 5 mM $MgCl_2$, 1 mM DTT). 26S Proteasomal activity was assessed by the addition of 10 μM of SUC-LLVY-AMC (Enzo Life Sciences). The contribution of 20S proteasomal activity was assessed by the comparison of 26S proteasome activity to that of total proteasome activity (26S+20S), measured by the activity of samples containing SDS at a final concentration of 0.05%.

Cell Culture Radiolabeling

Cortical neurons were cultured for 12 days in vitro. Radioactive labeling was done in Neurobasal growth media with B-27 supplement and without methionine or cysteine (Life Technologies, special order). ^{35}S methionine/cysteine (EasyTag PerkinElmer) was incorporated during indicated times at 55 mCi in the met/cys free growth medium. Where indicated, MG-132 (25 μM, Cell Signaling) and ATPγS (1 mM, Sigma) was added during the radioactive labeling window. For all labeling experiments, normal growth media on neurons was switched into labeling media supplemented with radioactive label for 10 minutes. Lysates were prepared in RIPA buffer (50 mM Tris pH 8.0, 150 mM NaCl, 1% Triton X-100, 0.5% Sodium Deoxycholate, 0.1% SDS, 5 mM EDTA, complete protease

inhibitor cocktail tablet (Roche), 1 mM sodium orthovanadate, 1 mM β-glycerophosphate). SDS sample buffer was added and samples were boiled for 5 minutes prior to loading onto SDS-PAGE gels. Autoradiographs were done by loading samples onto large SDS-PAGE gels, coomassie stained to verify equal loading, and then gels were dried down on a large gel drier onto Whatman filter paper. Dried gels were exposed to phosphorimager screens and scanned with a Typhoon FLA5500 imager.

Peptide collection and quantification

Following incorporation of radioactive ^{35}S methionine/cysteine, neurons were rapidly washed in PBS and fresh Neurobasal media without phenol red and with 2x B-27 supplement was added. At the two-minute time point, all of the media was collected and then spun through a 10 kDa Amicon filter (Millipore) and the flow through was then spun through a 3 kDa Amicon filter (Millipore). The flow-through from this sequential filtering was then dialyzed using dialysis tubing with a 100–500 Da cutoff (Spectrum Labs) into either 1x PBS (Gibco) or 20 mM Ammonium Bicarbonate (Sigma). Following four days of dialysis, samples were lyophilized and resuspended in MilliQ water for downstream calcium imaging. Quantification of peptides was done by counting the amount of radioactivity in each sample by liquid scintillation (Wallac 1410). Proteinase K control experiments were done by treating the media with 100 μg/mL proteinase K overnight in 2 M Urea and 10 mM BME, prior to re-dialyzing the proteolyzed media into 2 M Urea for two days, and then gradually reducing the Urea concentration down into NaCl and then into Ammonium Bicarbonate. Resuspended peptides were quantified prior to applications using LavaPep Fluorescent Peptide Quantification Kit (LP022010, Gel Company).

Biotin-epoxomicin

Biotin-epoxomicin is de-novo synthesized and purchased from Leiden University Institute of Chemistry. They are fully equipped with synthetic capabilities in organic chemistry. Mass spectrometry and NMR verify all batches produced by his lab for quality and purity. All batches used have had >99% purity. To further minimize batch variation, we test all batches in biological experiments (dose-titration for peptide release, NMP inhibition and cell viability responses).

Biotin-epoxomicin was added to neuronal cultures at 25 μM immediately after labeling. Following peptide release assays, treated cells were lysed in a sucrose homogenization buffer (0.32 M sucrose, 5 mM HEPES, 0.1 mM EDTA, 0.25 mM DTT). Membranes were separated from the cytosol by high-speed centrifugation at 55,000 RPM for 1 hour. Fractions were solubilized in SDS sample buffer prior to loading on SDS-PAGE gels for western analysis. EM processing was done after 5 minutes of treatment with Biotin-Epoxomicin.

Calcium imaging

Calcium imaging was performed as previously described[59]. Briefly, for the Biotin-Epoxomicin experiments, cultured embryonic cortical neurons were transfected with 1 μg of a mammalian expression construct encoding GCaMP3 at DIV10 and imaged at DIV 12–14. Bicuculline treatment was administered as a 1 μM stimulation in calcium imaging buffer in a perfusion setup. Once the bicuculline stimulation was washed out, biotin-epoxomicin (25

μM) was co-administered with 1 μM Bicuculline in calcium imaging buffer. Each treatment was monitored for three minutes prior to washout. Coverslips were not imaged twice due to Biotin-Epoxomicin being a covalent inhibitor. Cells were ensured to be healthy at the end of the imaging process by stimulating with 55 mM KCl and washing out and assessing for a proper calcium signal. Quantification was done by picking multiple regions of interests in primary and secondary dendrites across multiple coverslips over different imaging days. Data was analyzed using the Time Series Analyzer V3.0 ImageJ plugin and the ROI manager. Data were pooled for all the ROIs to generate a single N value. Brains from P0–P3 mouse pups (Cre-GCaMP3; Nestin-Cre ER) were dissected and plated in Neurobasal-A with B-27 supplement for two weeks. At DIV7, 4-hydroxytamoxifen (4-HT, concentration) was added to induce GCaMP expression. Neurons were imaged in a calcium-imaging buffer (130 mM NaCl, 3 mM KCl, 2.5 mM $CaCl_2$, 0.6 mM $MgCl_2$, 10 mM Hepes, 10 mM glucose, 1.2 mM $NaHCO_3$ pH 7.45). Peptides were collected, filtered, and dialyzed and then lyophilized prior to resuspension in 1 mL of MilliQ water and addition onto GCaMP-encoding neurons. 5 μl of resuspended peptides were sufficient to induce the described calcium-induced effects. Peptides treated with Proteinase K were spun through a 10 kDa MW cutoff filter prior to addition onto neurons in order to remove Proteinase K. Pharmacological inhibitors were perfused in at the indicated times at the following concentrations: BAPTA (2 μM), Thapsigargin (5 μM), Tetrodotoxin (1 μM), Nifedipine (1 μM), APV (2 μM).

Mass Spectrometry

Mass spectrometry for proteasomes isolated from cytosolic and membrane fractions was performed at MS Bioworks, LLC.

Statistics

No statistical methods were used to predetermine sample size. The experiments were not randomized. All statistical analyses were performed using Origin Prism and Graphpad software, accounting for appropriate distribution and variance to ensure proper statistical parameters were applied. Experimental sample sizes were chosen according to norms within the field. The observed magnitude of differences, together with the low replicate variance, permits high power of analysis based on the sample size chosen. For quantification of proteasomal localization by EM analysis, images were acquired by an independent assistant in the Johns Hopkins imaging core not involved in the experimentation and counts were then objectively tallied by a second assistant without knowledge of the experimental groups. Statistical methods used are described in figure legends for the respective EM experiments. For remaining experiments investigators were not blinded to allocation during experiments and outcome assessment. Statistical analysis using Student's *t* tests, 1-way ANOVAs and the appropriate post hoc tests were performed as described in each figure legend. *P* values ≤ 0.05 were considered significant.

Supplementary Material

Refer to Web version on PubMed Central for supplementary material.

Acknowledgments

We thank Dr. Sol H. Snyder, Dr. Xinzhong Dong, Dr. Jeremy Nathans, Dr. Geraldine Seydoux, Dr. Michael Caterina, Dr. Carolyn Machamer, Dr. Sin Urban, Dr. Zhe Li, Dr. Hana Goldschmidt, Kelsey Hopland, Chirag Vasavda, Anne Dietterich, Leah Cairns and members of the Margolis laboratory (Johns Hopkins University School of Medicine, Maryland) for valuable input, and reagents. Dr. Michael E. Greenberg (Harvard Medical School, Boston) for kindly providing EphB2 antibody. Special thanks to Bramwell Lambrus (Johns Hopkins University School of Medicine, Maryland). This work was funded by institutional funding and the following grants to S.S.M. (R01 MH102364). K.V.R. was supported by a training grant T32 GM007445 and NSF Graduate Research Fellowship DGE-1232825.

References

1. Coux O, Tanaka K, Goldberg AL. Structure and functions of the 20S and 26S proteasomes. Annu Rev Biochem. 1996; 65:801–847. DOI: 10.1146/annurev.bi.65.070196.004101 [PubMed: 8811196]
2. Ciechanover A. The ubiquitin-proteasome pathway: on protein death and cell life. Embo J. 1998; 17:7151–7160. DOI: 10.1093/emboj/17.24.7151 [PubMed: 9857172]
3. Ciechanover A, Schwartz AL. The ubiquitin-proteasome pathway: the complexity and myriad functions of proteins death. Proc Natl Acad Sci U S A. 1998; 95:2727–2730. [PubMed: 9501156]
4. Ben-Nissan G, Sharon M. Regulating the 20S proteasome ubiquitin-independent degradation pathway. Biomolecules. 2014; 4:862–884. DOI: 10.3390/biom4030862 [PubMed: 25250704]
5. Kisselev AF, van der Linden WA, Overkleeft HS. Proteasome inhibitors: an expanding army attacking a unique target. Chem Biol. 2012; 19:99–115. DOI: 10.1016/j.chembiol.2012.01.003 [PubMed: 22284358]
6. Ehlers MD. Activity level controls postsynaptic composition and signaling via the ubiquitin-proteasome system. Nat Neurosci. 2003; 6:231–242. DOI: 10.1038/nn1013 [PubMed: 12577062]
7. Wang HR. Regulation of cell polarity and protrusion formation by targeting RhoA for degradation. Science. 2003; 302:1775–1779. DOI: 10.1126/science.1090772 [PubMed: 14657501]
8. Karpova A, Mikhaylova M, Thomas U, Knopfel T, Behnisch T. Involvement of protein synthesis and degradation in long-term potentiation of Schaffer collateral CA1 synapses. J Neurosci. 2006; 26:4949–4955. DOI: 10.1523/JNEUROSCI.4573-05.2006 [PubMed: 16672670]
9. Dong C, Upadhya SC, Ding L, Smith TK, Hegde AN. Proteasome inhibition enhances the induction and impairs the maintenance of late-phase long-term potentiation. Learn Mem. 2008; 15:335–347. DOI: 10.1101/lm.984508 [PubMed: 18441292]
10. Djakovic SN, Schwarz LA, Barylko B, DeMartino GN, Patrick GN. Regulation of the proteasome by neuronal activity and calcium/calmodulin-dependent protein kinase II. J Biol Chem. 2009; 284:26655–26665. DOI: 10.1074/jbc.M109.021956 [PubMed: 19638347]
11. Bingol B, Schuman EM. Activity-dependent dynamics and sequestration of proteasomes in dendritic spines. Nature. 2006; 441:1144–1148. DOI: 10.1038/nature04769 [PubMed: 16810255]
12. Cai F, Frey JU, Sanna PP, Behnisch T. Protein degradation by the proteasome is required for synaptic tagging and the heterosynaptic stabilization of hippocampal late-phase long-term potentiation. Neuroscience. 2010; 169:1520–1526. DOI: 10.1016/j.neuroscience.2010.06.032 [PubMed: 20600658]
13. Rinetti GV, Schweizer FE. Ubiquitination acutely regulates presynaptic neurotransmitter release in mammalian neurons. J Neurosci. 2010; 30:3157–3166. DOI: 10.1523/JNEUROSCI.3712-09.2010 [PubMed: 20203175]
14. Wu S, et al. Cellular calcium deficiency plays a role in neuronal death caused by proteasome inhibitors. J Neurochem. 2009; 109:1225–1236. DOI: 10.1111/j.1471-4159.2009.06037.x [PubMed: 19476541]
15. Fonseca R, Vabulas RM, Hartl FU, Bonhoeffer T, Nagerl UV. A balance of protein synthesis and proteasome-dependent degradation determines the maintenance of LTP. Neuron. 2006; 52:239–245. DOI: 10.1016/j.neuron.2006.08.015 [PubMed: 17046687]
16. Pines J, Lindon C. Proteolysis: anytime, any place, anywhere? Nat Cell Biol. 2005; 7:731–735. DOI: 10.1038/ncb0805-731 [PubMed: 16056263]

17. Asano S, et al. Proteasomes. A molecular census of 26S proteasomes in intact neurons. Science. 2015; 347:439–442. DOI: 10.1126/science.1261197 [PubMed: 25613890]
18. Patrick GN, Bingol B, Weld HA, Schuman EM. Ubiquitin-mediated proteasome activity is required for agonist-induced endocytosis of GluRs. Curr Biol. 2003; 13:2073–2081. [PubMed: 14653997]
19. Blomen VA, et al. Gene essentiality and synthetic lethality in haploid human cells. Science. 2015; 350:1092–1096. DOI: 10.1126/science.aac7557 [PubMed: 26472760]
20. van Weering JR, et al. Intracellular membrane traffic at high resolution. Methods Cell Biol. 2010; 96:619–648. DOI: 10.1016/S0091-679X(10)96026-3 [PubMed: 20869541]
21. Chen X, et al. PSD-95 family MAGUKs are essential for anchoring AMPA and NMDA receptor complexes at the postsynaptic density. Proc Natl Acad Sci U S A. 2015; 112:E6983–6992. DOI: 10.1073/pnas.1517045112 [PubMed: 26604311]
22. Gazula VR, et al. Localization of Kv1.3 channels in presynaptic terminals of brainstem auditory neurons. J Comp Neurol. 2010; 518:3205–3220. DOI: 10.1002/cne.22393 [PubMed: 20575068]
23. Kim MJ, Dunah AW, Wang YT, Sheng M. Differential roles of NR2A- and NR2B-containing NMDA receptors in Ras-ERK signaling and AMPA receptor trafficking. Neuron. 2005; 46:745–760. DOI: 10.1016/j.neuron.2005.04.031 [PubMed: 15924861]
24. Hanley JG, Khatri L, Hanson PI, Ziff EB. NSF ATPase and alpha-/beta-SNAPs disassemble the AMPA receptor-PICK1 complex. Neuron. 2002; 34:53–67. [PubMed: 11931741]
25. Peebles CL, et al. Arc regulates spine morphology and maintains network stability in vivo. Proc Natl Acad Sci U S A. 2010; 107:18173–18178. DOI: 10.1073/pnas.1006546107 [PubMed: 20921410]
26. Lin DT, et al. Regulation of AMPA receptor extrasynaptic insertion by 4.1N, phosphorylation and palmitoylation. Nat Neurosci. 2009; 12:879–887. DOI: 10.1038/nn.2351 [PubMed: 19503082]
27. Ehlers MD. Reinsertion or degradation of AMPA receptors determined by activity-dependent endocytic sorting. Neuron. 2000; 28:511–525. [PubMed: 11144360]
28. Caterina MJ, Hereld D, Devreotes PN. Occupancy of the Dictyostelium cAMP receptor, cAR1, induces a reduction in affinity which depends upon COOH-terminal serine residues. J Biol Chem. 1995; 270:4418–4423. [PubMed: 7876207]
29. Zhu PP, et al. Cellular localization, oligomerization, and membrane association of the hereditary spastic paraplegia 3A (SPG3A) protein atlastin. J Biol Chem. 2003; 278:49063–49071. DOI: 10.1074/jbc.M306702200 [PubMed: 14506257]
30. Wunder C, Lippincott-Schwartz J, Lorenz H. Determining membrane protein topologies in single cells and high-throughput screening applications. Curr Protoc Cell Biol. 2010 Chapter 5, Unit 57.
31. Lee YC, Srajer Gajdosik M, Josic D, Lin SH. Plasma membrane isolation using immobilized concanavalin A magnetic beads. Methods Mol Biol. 2012; 909:29–41. DOI: 10.1007/978-1-61779-959-4_3 [PubMed: 22903707]
32. Smith MJ, Koch GL. Multiple zones in the sequence of calreticulin (CRP55, calregulin, HACBP), a major calcium binding ER/SR protein. Embo J. 1989; 8:3581–3586. [PubMed: 2583110]
33. Park S, et al. GDE2 promotes neurogenesis by glycosylphosphatidylinositol-anchor cleavage of RECK. Science. 2013; 339:324–328. DOI: 10.1126/science.1231921 [PubMed: 23329048]
34. Besche HC, Haas W, Gygi SP, Goldberg AL. Isolation of mammalian 26S proteasomes and p97/VCP complexes using the ubiquitin-like domain from HHR23B reveals novel proteasome-associated proteins. Biochemistry. 2009; 48:2538–2549. DOI: 10.1021/bi802198q [PubMed: 19182904]
35. Werner H, Dimou L, Klugmann M, Pfeiffer S, Nave KA. Multiple splice isoforms of proteolipid M6B in neurons and oligodendrocytes. Mol Cell Neurosci. 2001; 18:593–605. DOI: 10.1006/mcne.2001.1044 [PubMed: 11749036]
36. Fuchsova B, Fernandez ME, Alfonso J, Frasch AC. Cysteine residues in the large extracellular loop (EC2) are essential for the function of the stress-regulated glycoprotein M6a. J Biol Chem. 2009; 284:32075–32088. DOI: 10.1074/jbc.M109.012377 [PubMed: 19737934]
37. Zhang Y, et al. An RNA-sequencing transcriptome and splicing database of glia, neurons, and vascular cells of the cerebral cortex. J Neurosci. 2014; 34:11929–11947. DOI: 10.1523/JNEUROSCI.1860-14.2014 [PubMed: 25186741]

38. Vilchez D, et al. Increased proteasome activity in human embryonic stem cells is regulated by PSMD11. Nature. 2012; 489:304–308. DOI: 10.1038/nature11468 [PubMed: 22972301]
39. Schubert U, et al. Rapid degradation of a large fraction of newly synthesized proteins by proteasomes. Nature. 2000; 404:770–774. DOI: 10.1038/35008096 [PubMed: 10783891]
40. Kisselev AF, Akopian TN, Goldberg AL. Range of sizes of peptide products generated during degradation of different proteins by archaeal proteasomes. J Biol Chem. 1998; 273:1982–1989. [PubMed: 9442034]
41. Li N, et al. Relative quantification of proteasome activity by activity-based protein profiling and LC-MS/MS. Nat Protoc. 2013; 8:1155–1168. DOI: 10.1038/nprot.2013.065 [PubMed: 23702832]
42. Meng L, et al. Epoxomicin, a potent and selective proteasome inhibitor, exhibits in vivo antiinflammatory activity. Proc Natl Acad Sci U S A. 1999; 96:10403–10408. [PubMed: 10468620]
43. Patel TP, Man K, Firestein BL, Meaney DF. Automated quantification of neuronal networks and single-cell calcium dynamics using calcium imaging. J Neurosci Methods. 2015; 243:26–38. DOI: 10.1016/j.jneumeth.2015.01.020 [PubMed: 25629800]
44. Sato Y, Watanabe N, Fukushima N, Mita S, Hirata T. Actin-independent behavior and membrane deformation exhibited by the four-transmembrane protein M6a. PLoS One. 2011; 6:e26702. [PubMed: 22162747]
45. Besche HC, Goldberg AL. Affinity purification of mammalian 26S proteasomes using an ubiquitin-like domain. Methods in molecular biology. 2012; 832:423–432. DOI: 10.1007/978-1-61779-474-2_29 [PubMed: 22350902]
46. Tai HC, Schuman EM. Ubiquitin, the proteasome and protein degradation in neuronal function and dysfunction. Nat Rev Neurosci. 2008; 9:826–838. DOI: 10.1038/nrn2499 [PubMed: 18931696]
47. Tsvetkov P, et al. Operational definition of intrinsically unstructured protein sequences based on susceptibility to the 20S proteasome. Proteins. 2008; 70:1357–1366. DOI: 10.1002/prot.21614 [PubMed: 17879262]
48. Tsvetkov P, Reuven N, Prives C, Shaul Y. Susceptibility of p53 unstructured N terminus to 20 S proteasomal degradation programs the stress response. J Biol Chem. 2009; 284:26234–26242. DOI: 10.1074/jbc.M109.040493 [PubMed: 19617345]
49. Schmidt M, Finley D. Regulation of proteasome activity in health and disease. Biochim Biophys Acta. 2014; 1843:13–25. DOI: 10.1016/j.bbamcr.2013.08.012 [PubMed: 23994620]
50. Tai HC, Schuman EM. Ubiquitin, the proteasome and protein degradation in neuronal function and dysfunction. Nature reviews Neuroscience. 2008; 9:826–838. DOI: 10.1038/nrn2499 [PubMed: 18931696]
51. Jiang S, Dupont N, Castillo EF, Deretic V. Secretory versus degradative autophagy: unconventional secretion of inflammatory mediators. J Innate Immun. 2013; 5:471–479. DOI: 10.1159/000346707 [PubMed: 23445716]
52. Lee JG, Takahama S, Zhang G, Tomarev SI, Ye Y. Unconventional secretion of misfolded proteins promotes adaptation to proteasome dysfunction in mammalian cells. Nat Cell Biol. 2016; 18:765–776. DOI: 10.1038/ncb3372 [PubMed: 27295555]
53. Huh GS, et al. Functional requirement for class I MHC in CNS development and plasticity. Science. 2000; 290:2155–2159. [PubMed: 11118151]
54. Shatz CJ. MHC class I: an unexpected role in neuronal plasticity. Neuron. 2009; 64:40–45. DOI: 10.1016/j.neuron.2009.09.044 [PubMed: 19840547]
55. Xia Z, Dudek H, Miranti CK, Greenberg ME. Calcium influx via the NMDA receptor induces immediate early gene transcription by a MAP kinase/ERK-dependent mechanism. J Neurosci. 1996; 16:5425–5436. [PubMed: 8757255]
56. Nicoll RA, Roche KW. Long-term potentiation: peeling the onion. Neuropharmacology. 2013; 74:18–22. DOI: 10.1016/j.neuropharm.2013.02.010 [PubMed: 23439383]
57. Malenka RC, Nicoll RA. Long-term potentiation–a decade of progress? Science. 1999; 285:1870–1874. [PubMed: 10489359]
58. Margolis SS, et al. EphB-mediated degradation of the RhoA GEF Ephexin5 relieves a developmental brake on excitatory synapse formation. Cell. 2010; 143:442–455. DOI: 10.1016/j.cell.2010.09.038 [PubMed: 21029865]

59. Kim YS, et al. Central terminal sensitization of TRPV1 by descending serotonergic facilitation modulates chronic pain. Neuron. 2014; 81:873–887. DOI: 10.1016/j.neuron.2013.12.011 [PubMed: 24462040]

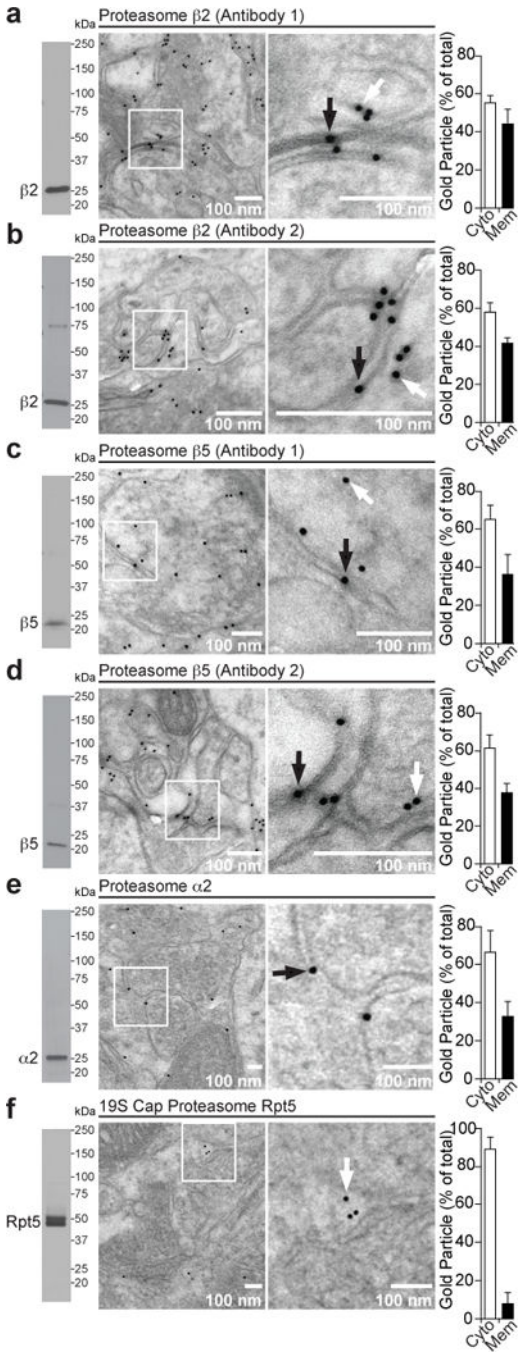

Figure 1. 20S proteasome subunits are localized to neuronal plasma membranes

(**a–f**) (left) Western blots of neuronal lysates probed using indicated antibodies. (**a–f**) (center) Electron micrographs of immunogold labeling (12 nm gold particles) from hippocampal slice preparations using antibodies raised against core catalytic β2 (**a, b**), β5 (**c, d**), α2 (**e**) proteasomal subunits and 19S cap proteasome subunit Rpt5 (**f**). Representative images shown. White boxes on EM show magnified region (displayed to the right). Several arrows shown corresponding to immunogold label; cytosolic (white); membrane (black). (**a–f**) (Right) Quantification of gold particles from cytosol (Cyto) and membrane (Mem). N

number of micrographs were quantified to get at least 300 gold particles: **a**) N=49; **b**) N=47; **c**) N=43; **d**) N=54; **e**) N=54; **f**) N=92. >300 gold-particles per antibody were counted. Slices were made from two separate 3-month old mice, >20 slices were generated for immuno-EM analysis. Data are presented as mean ± SEM. Source data are available online.

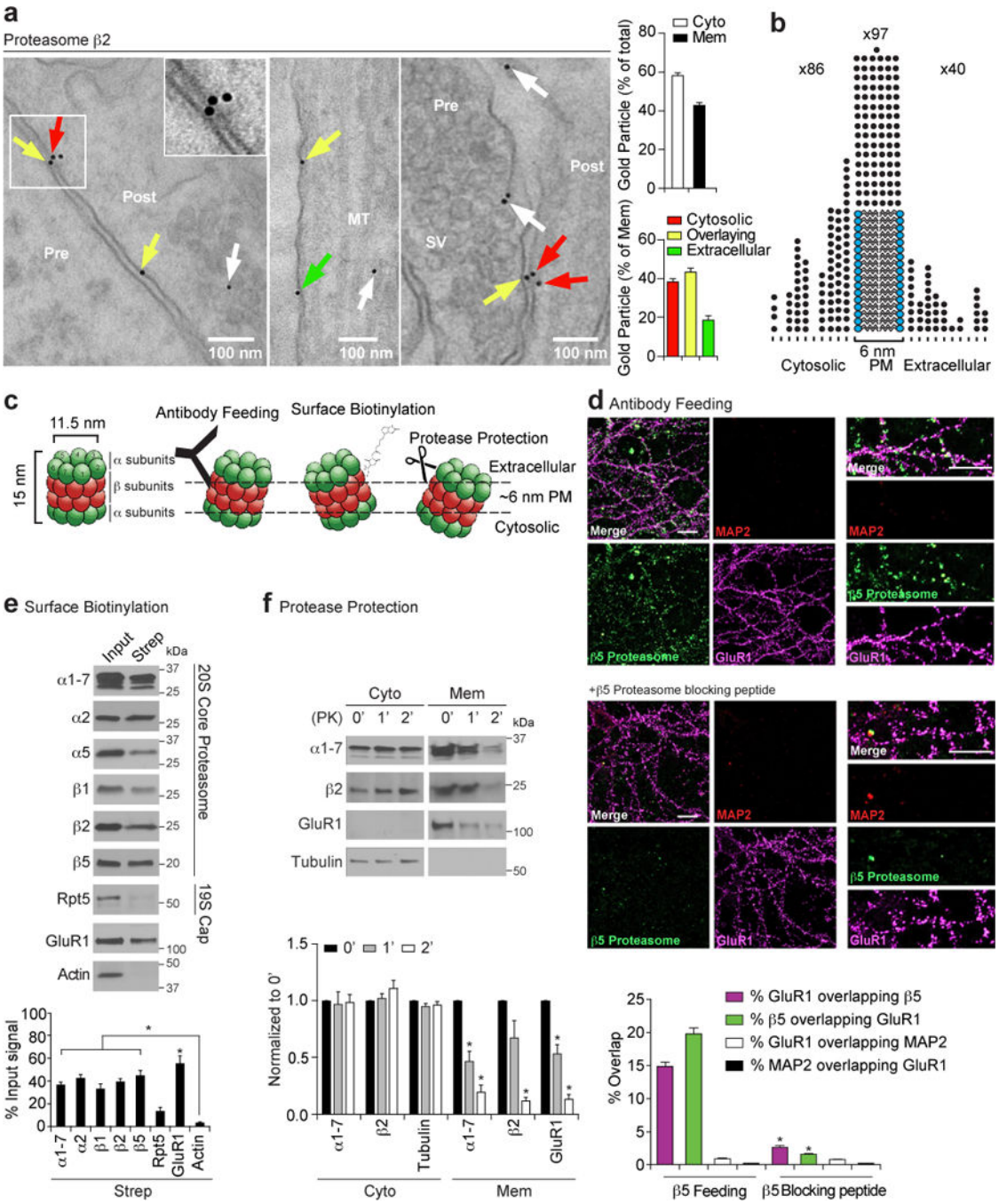

Figure 2. Neuronal membrane proteasomes are exposed to the extracellular space

(**a**) Electron micrographs of immunogold labeling (12 nm gold particles) from DIV14 primary mouse cortical neuronal cultures using β2 antibody. Representative images shown. Inset shows magnified region. Ultrastructures: Presynaptic (Pre); Postsynaptic (Post); Microtubules (MT); Synaptic vesicles (SV). Arrows: cytosolic (white); membrane (red-cytosolic face), (yellow-overlaying), (green-extracellular face). (N=84 images, >300 gold-particles. Multiple punches from single culture, >20 slices generated). Quantification to right. (**b**) Quantification depicted for a subset of gold particles near membranes. Each tick

mark represents 2 nm from the plasma membrane (PM). Each dot represents a single gold particle, totals shown above (**c**) Schematic showing three different approaches to determine whether proteasomes were surface-exposed. (**d**) Antibody Feeding: Live primary mouse DIV14 cortical neuronal cultures were incubated with antibodies against MAP2, N-terminus of GluR1 (GluR1), or β5 proteasome subunits. Representative images shown, scale bar = 10 μM. β5 antibody pre-incubated with the blocking peptide shown below. Quantification of percentage overlap shown (N=2 independent neuronal cultures, n=15 neurons/culture). Significance is calculated between β5 antibody and β5 antibody pre-incubated with blocking peptide. **P*<0.01 (two-tailed Student's *t*-test). (**e**) Surface biotinylation: Proteins from surface biotinylated DIV14 cortical neurons were precipitated on streptavidin affinity beads and immunoblotted. Representative immunoblots of input lysates (~3.5% of total, left) and streptavidin pulldown of lysates (Strep) (~11% of total, right). Quantification is of streptavidin signal normalized to input signal (N=4 independent neuronal cultures). **P*<0.01 (one-way ANOVA). (**f**) Protease Protection: Proteinase K (PK) was applied onto DIV14 cultured cortical neurons for indicated times. Cytosolic (Cyto) and membrane (Mem) fractions were immunoblotted. Quantification is below. Significance for each timepoint against the zero minute timepoint is calculated (N=3 independent neuronal cultures). **P*<0.01 (two-tailed Student's *t*-test). All data are presented as mean ± SEM. Uncropped blots shown in Supplementary Data Set 1. Source data available online.

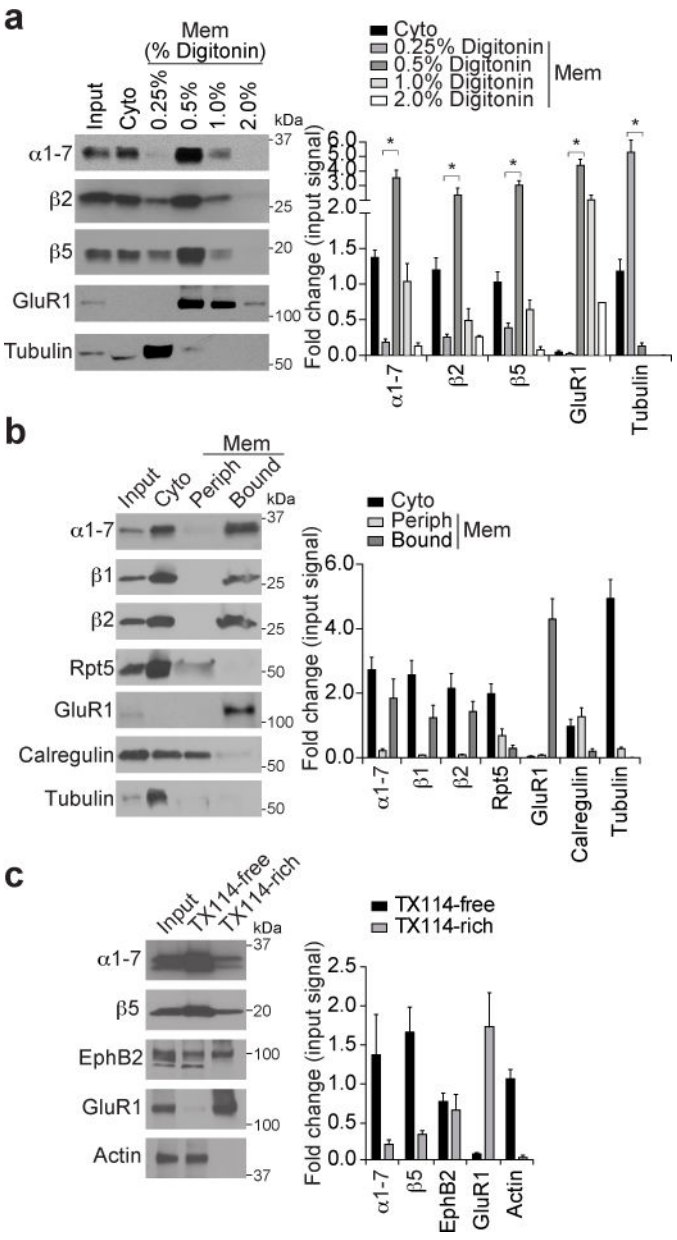

Figure 3. Neuronal membrane proteasomes are tightly associated with plasma membranes

(**a**) Primary mouse cortical neuronal cultures at DIV 14 were fractionated into cytosolic (Cyto) and membrane (Mem) components. Membranes were extracted with indicated sequentially increasing concentrations of Digitonin. Samples were analyzed by immunoblotting using antibodies against indicated proteins. Quantification to the right is normalized to input signal levels for each antibody. While 0.25% digitonin extracted cytosolic protein Tubulin, higher concentrations (0.5%, 1.0%) of digitonin were required to extract known hydrophobic proteins such as GluR1. An explanation of percentages loaded on gel is explained in materials and methods. Significance is calculated by comparing signal from the 0.5% digitonin fraction to the 0.25% digitonin fraction for each antibody (N=3 independent neuronal cultures). **P*<0.01 (one-way ANOVA). Data are presented as mean ±

SEM. (**b**) Proteasome subunits are tightly bound to membranes. Neuronal cultures at DIV14 were fractionated into cytosolic, peripherally-associated (Periph), and tightly-bound (Bound) proteins. Immunoblots of each fraction using indicated antibodies are shown. Quantification to right, data are presented as mean ± SEM (N=3 independent neuronal cultures). (**c**) Cultured neurons at DIV14 were phase separated with TX-114 (TX114). Immunoblots shown using indicated antibodies. TX114-free indicates aqueous phase, and TX114-rich contains the TX-114 phase. Quantification to the right, data are presented as mean ± range (N=2 independent neuronal cultures). Uncropped blots are shown in Supplementary Data Set 1. Source data are available online.

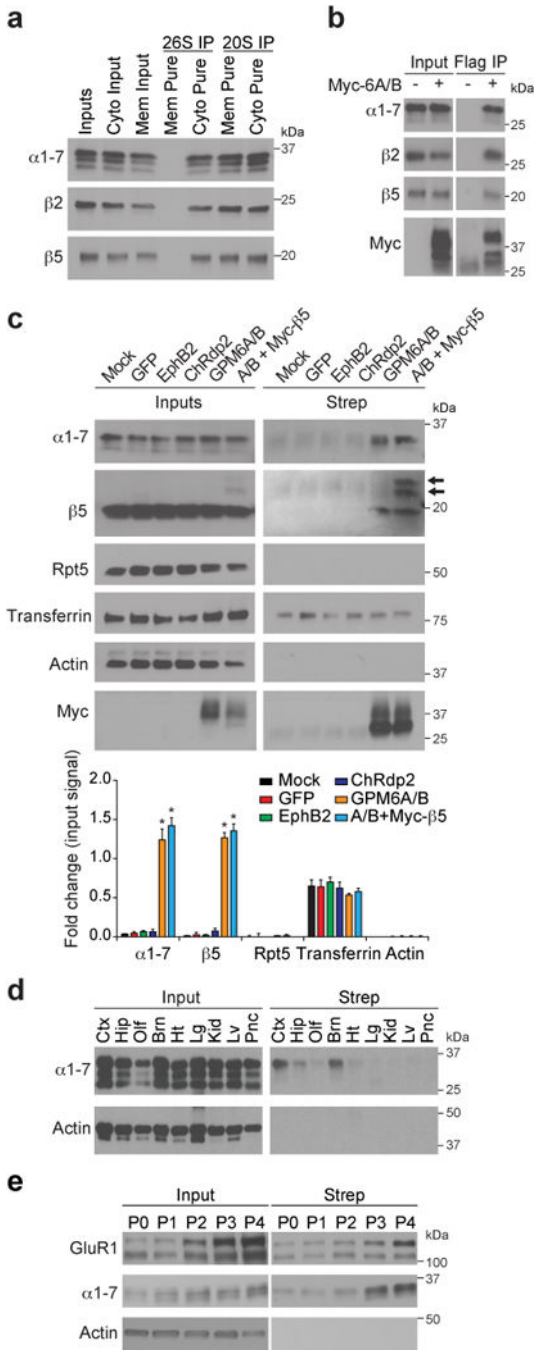

Figure 4. Neuronal membrane proteasomes are largely a 20S proteasome and in complex with GPM6 family glycoproteins

(**a**) Representative immunoblots of proteasomes purified out of neuronal cultures using capped-26S (26S IP) or 20S purification matrices (20S IP). Purification (Pure) was done out of either neuronal cytosol (Cyto) or detergent-extracted neuronal plasma membranes (Mem). (**b**) Immunoprecipitation with anti-Flag from HEK293 cell lysates previously transfected with plasmids containing Myc/Flag tagged GPM6A and GPM6B, followed by immunoblotting with Myc or proteasome antibodies (α1–7, β2, β5). Inputs (10% of total,

left) and immunoprecipitated samples (75% of total, right) are shown. (**c**) Exogenous expression of GPM6A/B is sufficient to induce surface expression of endogenous proteasomes in HEK293 cells. HEK293 cells were mock transfected (Mock) or transfected with plasmids containing GFP, EphB2, Channelrhodopsin-2 (ChRdp2), GPM6A/B, and GPM6A/B + Myc-tagged β5 (A/B+Myc-β5). Cells were surface biotinylated. Representative immunoblots of input lysates (4% of total, left) and streptavidin pulldowns of lysates (32% of total, right). Quantification shown below is normalized to input signal. β5 western is overexposed in order to see Myc-tagged bands (two arrows, right of immunoblot). Significance is calculated compared to A/B transfected samples (N=3 independent cell cultures and transfections). **P*<0.01, one way ANOVA. Data are presented as mean ± SEM. (**d**) Surface-exposed proteasome expression is unique to nervous system tissues. Tissues from P3 mouse were surface biotinylated. Cortex (Ctx), Hippocampus (Hip), Olfactory bulb (Olf), Hind Brain (Brn), Heart (Ht), Lung (Lg), Kidney (Kid), Liver (Lv), Pancreas (Pnc). Representative immunoblots of input lysates (2% of total, left) and streptavidin pulldowns of lysates (4% of total, right). (**e**) Representative western blots of input lysates (2.5% of total, left) and streptavidin pulldown (7.5% of total, right) of biotinylated proteins following surface biotinylation of mouse cortex tissue dissected from indicated postnatal ages. Uncropped blots shown in Supplementary Data Set 1. Source data available online.

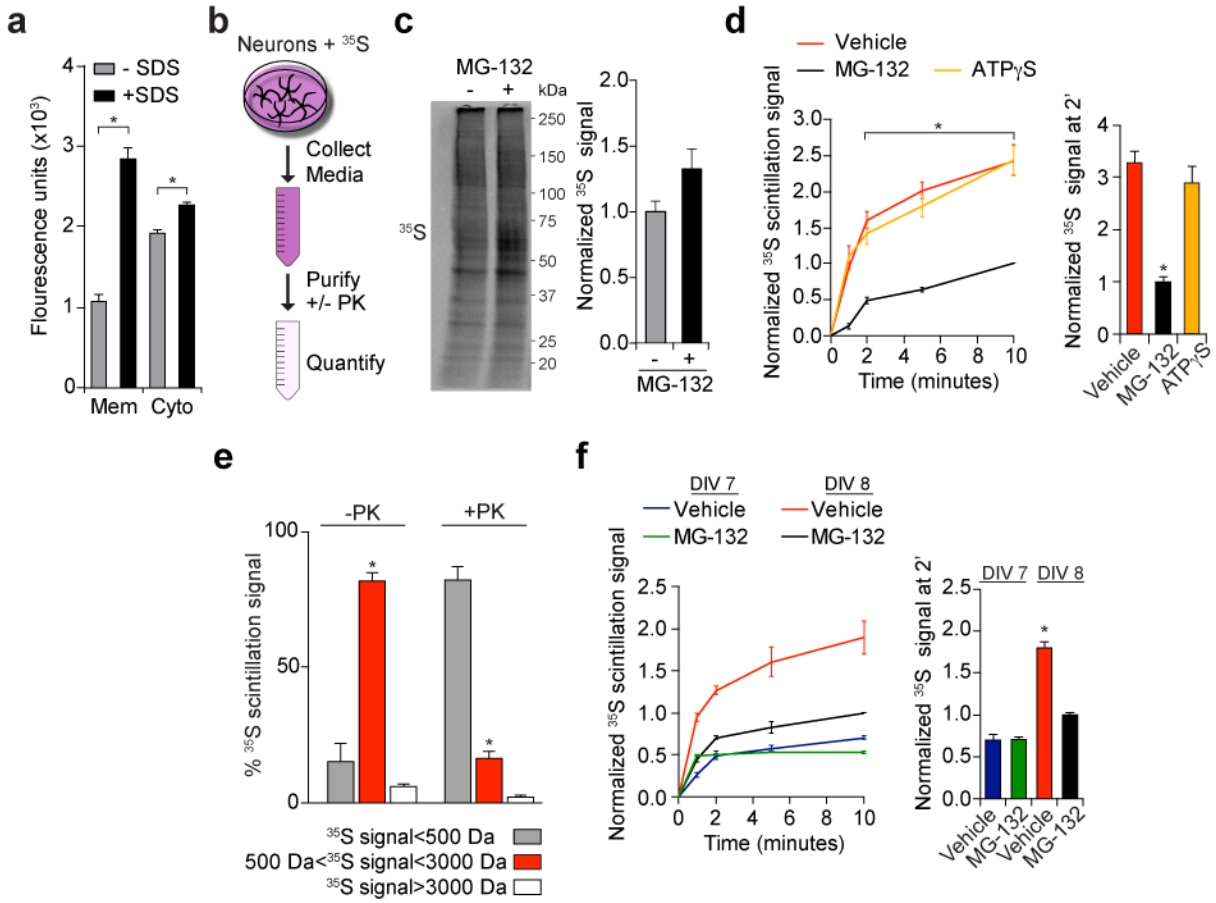

Figure 5. Neuronal membrane proteasomes degrade intracellular proteins into extracellular peptides

(**a**) Purified 20S proteasomes from neuronal cytosol (Cyto) or membrane (Mem) were incubated with the fluorogenic proteasome peptide substrate SUC-LLVY-AMC. Endpoint fluorescence with and without incubation with SDS (.02%) is quantified. Significance is shown between SDS-treated and untreated samples (N=3 proteasome purifications, independent neuronal cultures). (**b**) Schematic for collection and purification of extracellular peptides. Media collected from neurons following radiolabeling was subjected to size exclusion purification, with or without Proteinase K (PK). (**c**) Representative autoradiograph of lysates from cortical neurons previously radiolabeled with ^{35}S methionine/cysteine for 10 minutes in the presence or absence of MG-132. Quantification of signal normalized to vehicle-treated neurons is shown (right). (**d**) Rapid efflux of radioactive material out of neuronal cultures into media depends upon proteasome function. Media collected from neurons following radiolabeling with or without MG-132 or ATPγS. Liquid scintillation quantification of media at indicated timepoints is shown normalized to MG-132 at 10-minute timepoint; 2 minute timepoint shown separately on bar graph (right) (Media from N=3 independent neuronal cultures). Significance in line graph is shown for MG-132 treated neurons compared to vehicle alone at each time point. (**e**) Media collected from neurons following radiolabeling was subjected to size exclusion purification, with or without Proteinase K (PK). The percentage of total radioactivity eluting at different sizes is shown (N=3 independent neuronal cultures and purifications). (**f**) Release of proteasome-derived

peptides in the extracellular space correlates with NMP expression. Experiment performed as described in (**d**); media collected from either DIV7 or DIV8 neurons, with MG-132 (MG-132) or without (Vehicle). (Media of N=2 independent neuronal cultures) *P<0.05 ((**a**, **e, f**) two-tailed Student's t-test, (**e**) significance of 500<^{35}S Signal<3000Da compared to <500Da and >3000Da; (**d**) One-way ANOVA). Data are mean ± SEM (**a,c,d,e**) or ± range (**f**). Source data available online.

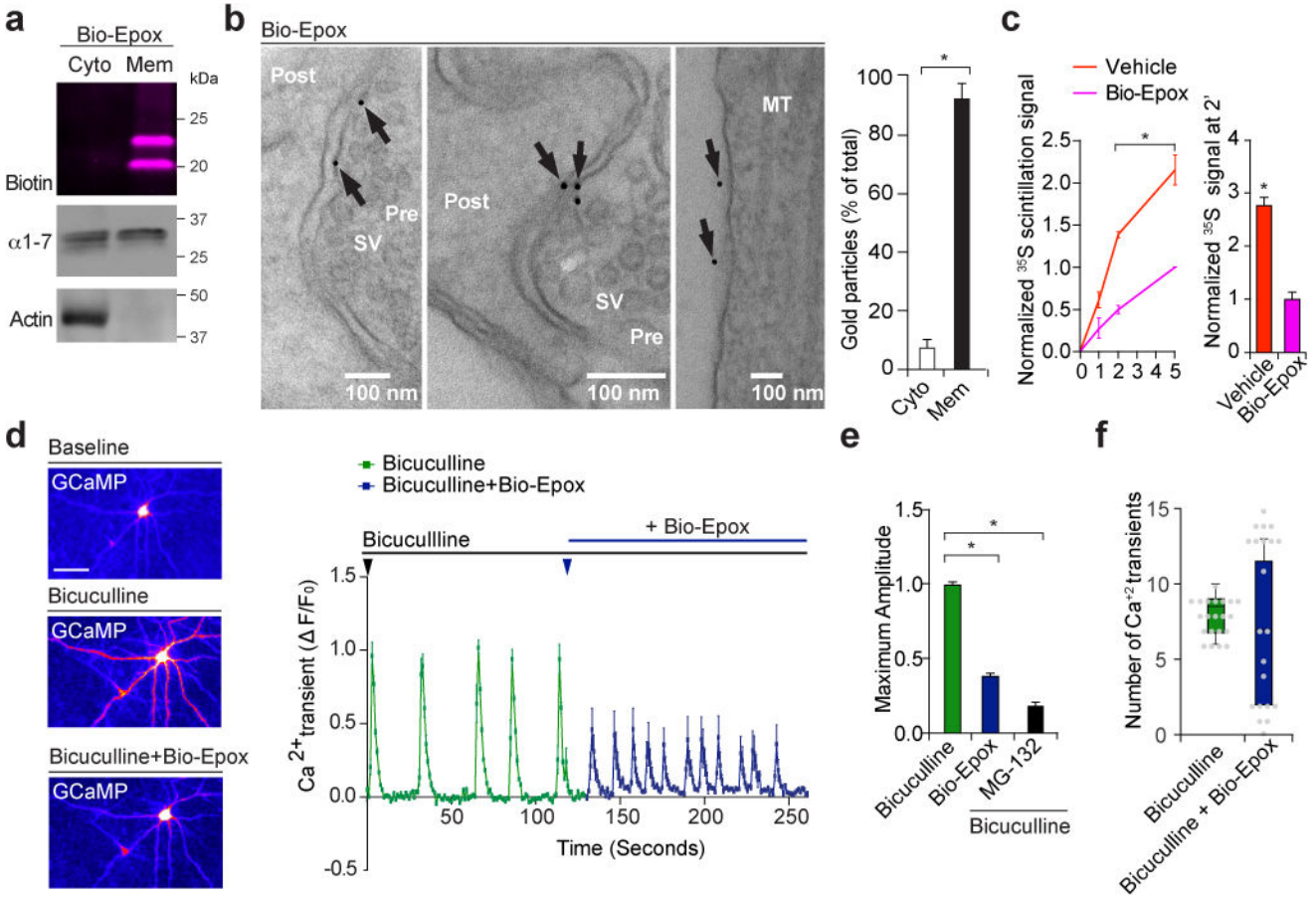

Figure 6. Neuronal membrane proteasomes are required for release of extracellular peptides and modulate neuronal activity

(**a,b**) Biotin-epoxomicin does not cross neuronal membranes and covalently modifies proteasome subunits. (**a**) Neurons treated with biotin-epoxomicin (Bio-Epox) were separated into cytosolic (Cyto) and membrane (Mem) fractions and analyzed by western using streptavidin conjugated to a fluorophore. Immunoblots using indicated antibodies shown below. (**b**) Immunogold labeling against biotin using streptavidin-Au (black arrows) from neuronal cultures treated with Bio-Epox, with representative images shown. (N=54, obtained from multiple punches of a single neuronal culture, >20 slices generated.) Labeled ultrastructures: Presynaptic regions (Pre), Postsynaptic regions (Post), Microtubules (MT), and synaptic vesicles (SV). Quantification of particles in cytosol and on membrane (right). (**c**) Specific inhibition of neuronal membrane proteasomes blocks release of extracellular peptides. Media collected from radiolabelled neurons treated with Bio-Epox or without (Vehicle). Liquid scintillation quantification of media at indicated timepoints is shown normalized to Bio-Epox at the 5 minute timepoint; 2 minute timepoint shown separately. Significance is shown for Bio-Epox treated neurons compared to vehicle alone. (N=3 independent neuronal cultures). (**d**) NMP inhibition modulates speed and intensity of neuronal calcium transients. Bicuculline added (downward black arrowhead) to naïve GCaMP3-encoding neurons. Downward dark blue arrowhead indicates timing of Bio-Epox addition. Representative images (left) and traces of Bicuculline response before and after

Bio-Epox addition are plotted (right). Scale bar = 40 μM. Quantification of normalized fluorescence intensity ($\Delta F/F_0$) measurements of calcium signals over imaging timecourse are shown. (**e**) Average maximum amplitudes are plotted, and include analysis of calcium signaling after treatment with MG-132. Significance compared to Bicuculline stimulation alone. (**f**) Box-and-whisker plot of all frequencies observed. *P<0.05, one-way ANOVA (E), two-tailed Student's t-test (B,C). All data are presented as mean ± SEM (D-F, N=2 independent replicate cultures, n=24 neurons per culture, with 18 ROIs (regions of interest) analyzed per neuron). Uncropped blots shown in Supplementary Data Set 1. Source data available online.

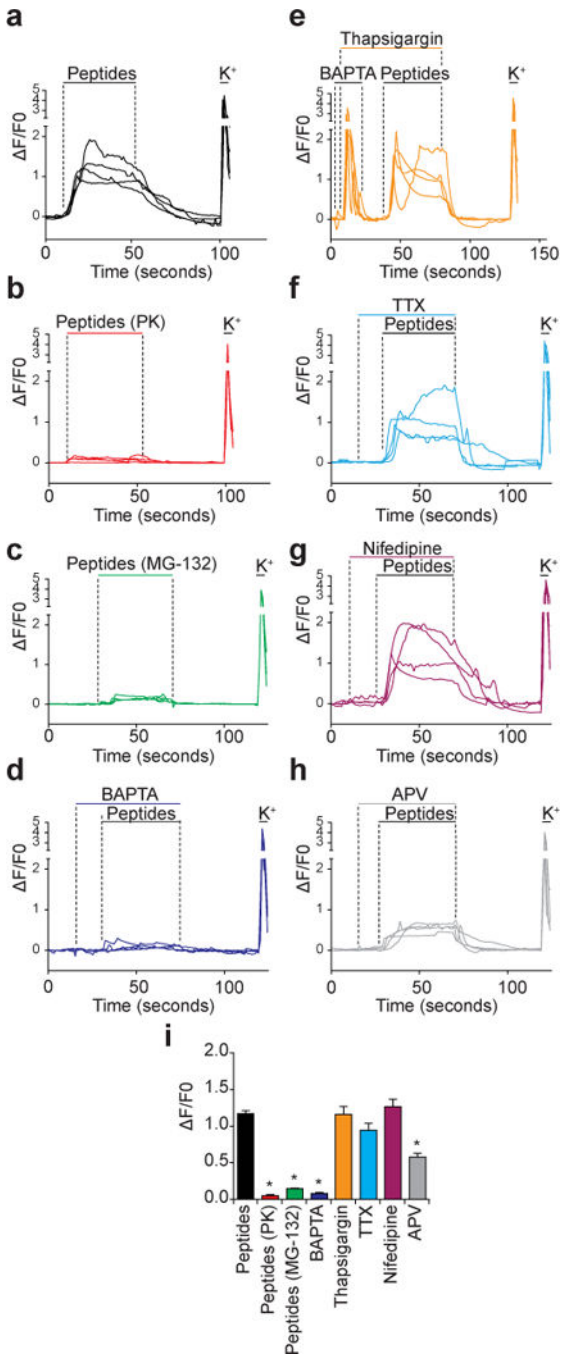

Figure 7. Neuronal membrane proteasome-derived peptides are sufficient to induce neuronal signaling

(**a**) Purified peptides were perfused onto GCaMP3-encoding mouse cortical cultured neurons. Dotted lines indicate time of peptide addition and washout. K^+ indicates the timing of 55 mM KCl addition to neurons to determine that they still respond properly at the end of the experiment. Line graph shows increase in fluorescence over baseline during time of peptide addition, a decrease following washout and robust increase with KCl addition. Four sample traces from different neurons are plotted. (**b, c**) Similar to part (**a**), cultured neurons

were incubated with either Peptides (PK) (peptides were pretreated with P K, PK was removed, and then samples dialyzed to remove small molecules) or with Peptides (MG-132) (peptides purified from cells treated with MG-132). (**d**–**h**) Indicated drugs were perfused onto neuronal cultures during the times depicted by the dashed lines. Peptides were subsequently added as indicated and described in (**a**). Concentrations of drugs: BAPTA (2 μM), Thapsigargin (5 μM), Tetrodotoxin (1 μM), Nifedipine (1 μM), APV (2 μM). (**i**) Quantification of maximum intensity of change from each condition is plotted. **P*<0.01 one-way ANOVA. Data are presented as mean ± SEM (N=3 independent replicate cultures, n>15 neurons per treatment, with at least 10 ROIs analyzed per neuron, per condition). Source data available online.

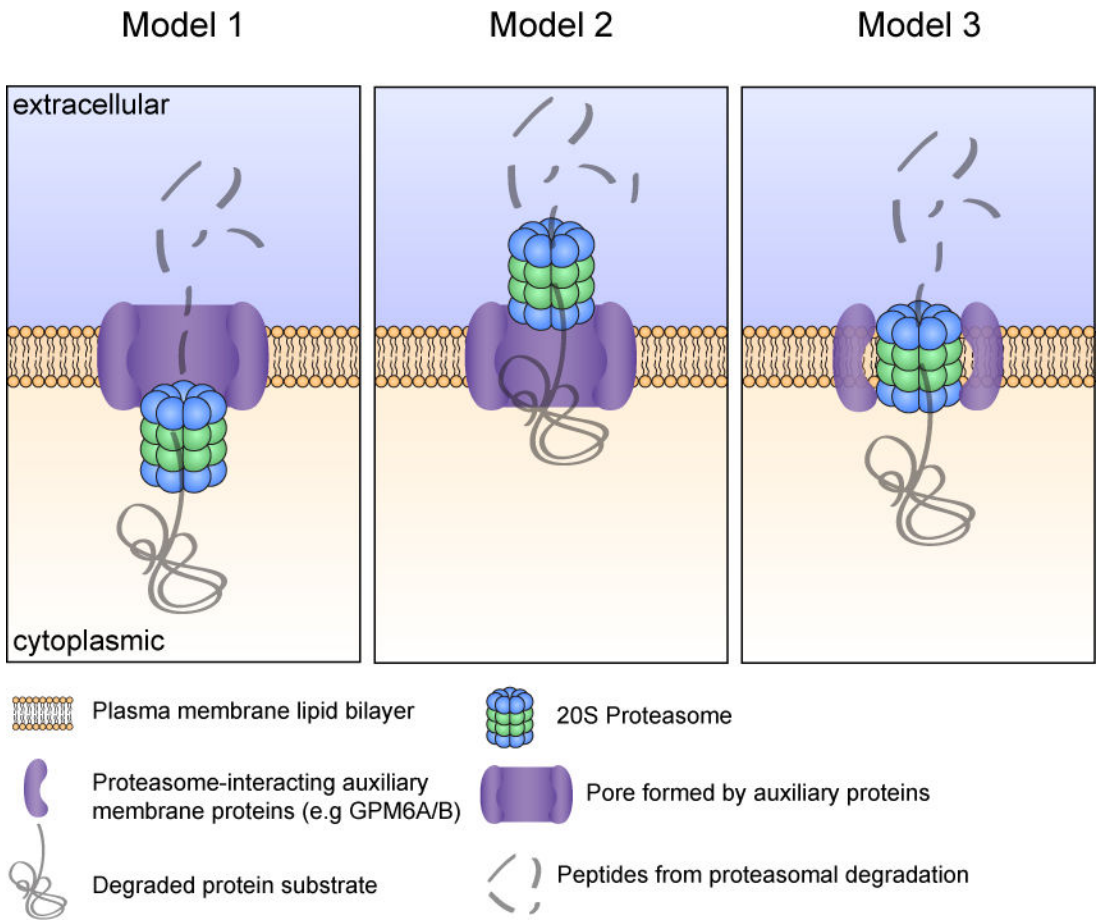

Figure 8. Proposed theoretical models of NMP association with the plasma membrane

Three models of how proteasomes can associate with plasma membranes are shown above. Extracellular and cytoplasmic sides of the plasma membrane are indicated. Symbol key shown below.